NETWORKS AND HETEROGENEOUS MEDIA
©American Institute of Mathematical Sciences
Volume **8**, Number **1**, March **2013**
doi:10.3934/nhm.2013.8.343
pp. **343–378**

WAVESPEED SELECTION IN THE HETEROGENEOUS FISHER EQUATION: SLOWLY VARYING INHOMOGENEITY

John R. King

School of Mathematical Sciences
University of Nottingham
Nottingham, NG7 2RD, England

Abstract. We adapt (ray-based) geometrical optics approaches to encompass the formal asymptotic analysis of front propagation in a Fisher-KPP equation with slowly varying spatial inhomogeneities. The wavespeed is shown to be selected by two distinct (and fully constructive) mechanisms, depending on whether the source term is an increasing or decreasing function of the spatial variable. Canonical inner problems, analogous to those arising in the geometrical theory of diffraction, are formulated to give refined expressions for the wavefront location. Additional phenomena, notably the initiation of new fronts and the transitions that occur when the source term is a non-monotonic function of space, are shown to be amenable to the same asymptotic approaches.

1. **Introduction.** A key question in characterising wave propagation over an unstable state is associated with determining the speed at which such propagation occurs. A very well-studied (and comparatively simple) representative example is provided by the Fisher-KPP equation

$$\frac{\partial u}{\partial t} = \frac{\partial^2 u}{\partial x^2} + u(1-u), \ -\infty < x < +\infty, \tag{1}$$

whereby a localised perturbation (compactly supported, say) with $u > 0$ to the unstable uniform state $u \equiv 0$ generates waves of asymptotic (i.e. large-time) speed $c = 2$ propagating in both directions, between which the stable state $u = 1$ is established. That the speed can be expected to be given by $c = 2$ can be established heuristically either from the phase plane for the associated travelling-wave ordinary differential equation (see (11) below), as the minimum speed for which a non-negative heteroclinic connection between $u = 1$ and $u = 0$ exists, or by linearising the PDE about $u = 0$ to obtain

$$u \sim \frac{M}{2\sqrt{\pi t}}\, e^{t-x^2/4t}$$

for some constant M as the intermediate asymptotic behaviour, from which it is readily observed that the condition for the linearisation to be applicable as $t \to \infty$ can be expressed as $|x|/t > 2$. That $c = 2$ applies here has long been established

2010 *Mathematics Subject Classification.* Primary: 35K57; Secondary: 35C20.
Key words and phrases. Reaction-diffusion, wave propagation, ray methods, asymptotic analysis.

rigorously, with many refinements of the result also in place[1]. A motivation for the current work was, nevertheless, to gain more intuitive understanding of why each of these heuristic arguments gives the same answer and, indeed, why that answer is the correct one. In doing this, it proves instructive to consider a direct spatially heterogeneous generalisation of (1), namely (2) below; with this generalisation, we find that arguments analogous to the two above in general give different answers, having complementary and all-encompassing regimes of applicability. Thus we identify two distinct mechanisms for wavespeed selection that we term the repeated-root mechanism and the Hamilton-Jacobi mechanism and which we believe are of much broader applicability; while each is based on linear arguments (associated with linearisation either of the travelling-wave reduction or of the PDE itself), each gives a fully constructive method for determining the wavespeed of the associated nonlinear problem within its regime of applicability: the repeated-root condition involves identification of the minimum speed within the travelling-wave phase plane by determining the condition for a degenerate node, while the Hamilton-Jacobi case involves (in its simplest guise) the construction of the expansion-fan solution of the relevant eikonal equation. To exemplify the lessons that we claim can be learnt from such an analysis, we highlight straightaway the implications that conclusions arising from a phase-plane analysis (or from the linearisation of the PDE) alone must be treated with considerable caution, despite the intuitive appeal of such a simplification, and that ray methods of the type pioneered in linear problems (geometrical optics in particular[2]) have a considerable amount to say about nonlinear ones of the type we address here and whose broader application, given that they have been underexploited in such contexts, we advocate.

The current paper thus concerns the Cauchy problem for the heterogeneous monostable reaction-diffusion equation (we refer to [11] for a review of past studies of such systems, while noting that there are also many more recent investigations)

$$\varepsilon\frac{\partial u}{\partial t}=\varepsilon^2\frac{\partial^2 u}{\partial x^2}+\Psi(x)u\left(1-u/\Phi(x)\right)\ \text{ for } -\infty<x<+\infty, \tag{2}$$

for $u(x,t)$ with initial conditions

$$\text{at } t=0 \quad u=u_I(x;\varepsilon),$$

wherein $\Psi,\Phi>0$ and $u_I\geq 0$ for all x. We are concerned here with the regime $0<\varepsilon\ll 1$, so taking Ψ and Φ to be independent of ε amounts to an assumption that the heterogeneity in the source term is spatially slowly varying. We remark that the nonlinearity in the source term could readily be generalised but that we shall focus on the above (Fisher-like) form in order to avoid issues of nonlinear selection (pushed fronts[3]) that would be a distraction in the current context – we refer to [2] for the relevant background and references and for analysis that is complementary to what follows here[4]; directly relevant earlier work of which we were unaware

[1] With apologies, we forego here any attempt to give a proper account of the very extensive relevant literature; a valuable way in is provided by [10].

[2] See [5], for example, for background on linear waves, including on associated terminology adopted below.

[3] For nonlinearities for which a pushed front arises, the travelling-wave solution with $c=2$ has u passing through zero before tending back to zero from below, so that the minimal admissible wavespeed has $c>2$ and its calculation requires global rather than local phase-plane analysis.

[4] [2] focusses on detailed analysis of cases involving power-law $\Psi(x)$; our investigations here will be less concrete but more general. In the interests of making the current discussion relatively self-contained we shall, however, revisit some of the results of [2].

while writing [2] includes that of Freidlin, e.g. [6], Evans and Souganidis [4] and Méndez et al. [9]; in particular, Example 2 of [6] is very close to one of those discussed in [2]. As already implied, in the interests of brevity we shall not include a detailed literature review here nor shall we discuss natural generalisations of (2) that can fairly readily be analysed by the methods outlined below, including the multidimensional case (see Section 7 of [2], however) and cases

$$\varepsilon\frac{\partial u}{\partial t}=\varepsilon^2\frac{\partial}{\partial x}\left(D(x)\frac{\partial u}{\partial x}\right)+S(u,x)$$

in which the diffusivity is also non-uniform.

For ease of exposition we shall take

$$\Psi(0)=\Phi(0)=1 \tag{3}$$

and, where relevant, assume

$$\lim_{x\to+\infty}\Psi(x)=\Psi_\infty, \tag{4}$$

for some positive constant Ψ_∞. We shall require $u_I(x;\varepsilon)$ to decay sufficiently rapidly to zero at $|x|\to\infty$ that the minimum wavespeed is realised (and in particular to be exponentially small in ε for $|x|\gg\varepsilon$; we make more precise statements in due course), on obvious symmetry grounds discuss the behaviour in $x>0$ only and focus primarily on Ψ being monotonic in x, the cases $\Psi'>0$ and $\Psi'<0$ exhibiting significantly different behaviour. Importantly for what follows, the linearised version of (2) (linearised about $u=0$) is of course independent of $\Phi(x)$.

Our main goal here is to determine the propagation speed associated with (2), which could be defined as the location $x=s(t;\varepsilon)$ at which

$$u\left(s(t;\varepsilon),t\right)=\frac{1}{2}\Phi\left(s(t;\varepsilon),t\right), \tag{5}$$

say, whereby as $t\to+\infty$

$$\begin{aligned} &u\left(x,t\right)\to\Phi(x)\text{ as }\varepsilon\to0\text{ for }0<x/s<1,\\ &u(x,t)\to0\quad\text{for }x/s>1, \end{aligned} \tag{6}$$

for each fixed x/s. For practical reasons, our subsequent working definition of s will differ somewhat from (5), but (6) will remain valid.

Approaches based on geometric optics are relatively rarely applied to parabolic problems, but will be essential to the formal methods described here: we highlight the pioneering work of Cohen and Lewis [1] on applications to linear parabolic equations, as well as that of Freidlin and coworkers (e.g. [6]) on approaches based on large-deviation theory, and also mention [7], [8] as earlier examples of the application of the current formal techniques in determining the tail behaviour of nonlinear problems. In many places our analysis will need to go beyond geometrical optics, however, by formulating and analysing canonical inner problems analogous to those arising in the geometrical theory of diffraction: these analyses will enable us to establish formally a number of results that we believe to warrant subsequent rigorous treatment.

The remainder of the paper is organised as follows (note that the same notation is often used with different meanings in different sections); for the most part we limit ourselves to discussion of monotonic $\Psi(x)$. In Section 2 we study the two early timescales $t=O(\varepsilon)$ and $t=O(\varepsilon^{1/3})$ that are required to provide a comprehensive asymptotic description of (2) in the limit $\varepsilon\to0$ and which provide valuable insight

into the analysis of the main timescale $t = O(1)$ in Sections 3 (mechanisms for wavespeed selection), 4 (initiation of additional wavefronts) and 5 (other related matters). Section 6 provides discussion, while Appendix 1 identifies a distinguished limit in which Ψ is almost uniform that captures the transition between the distinct wavespeed-selection mechanisms. Appendix 2 analyses a perceptive example from [6] in which Ψ is piecewise constant, making the problem particularly susceptible to detailed calculation; Appendix 3 outlines a canonical inner problem associated with Appendix 2.

2. **The early time behaviour.**

2.1. $\boldsymbol{t = O(\varepsilon)}$.

For the purposes of this section we take

$$\Psi(x) \sim 1 + \lambda x + \mu x^2 \quad \text{as } x \to 0. \tag{7}$$

The only non-generic case we shall consider here is $\Psi(x) \equiv 1$ and we could otherwise without loss of generality take $|\lambda| = 1$ in (7), with $\lambda = 1$ corresponding to $\Psi'(x) > 0$ and $\lambda = -1$ to $\Psi'(x) < 0$. We also take

$$u_I(x;\varepsilon) = U_I(X)$$

with $x = \varepsilon X$ and where U_I will be taken to decay much more rapidly than $\exp(-X)$ as $X \to +\infty$ in order to ensure that the minimum wavespeed is realised.

The first timescale has $t = \varepsilon T$, whereby at leading order in ε we have the classical (Fisher) problem

$$\frac{\partial u_0}{\partial T} = \frac{\partial^2 u_0}{\partial X^2} + u_0(1 - u_0), \tag{8}$$
$$\text{at } T = 0 \quad u_0 = U_I(X),$$

where we have used (3). The large-time behaviour of (8) in $X > 0$ takes the familiar form

$$u_0 \sim \phi(z;2) \quad \text{as} \quad T \to +\infty \quad \text{with} \quad z = O(1) \tag{9}$$

where

$$z = X - 2T + \frac{3}{2}\ln T + z_0 \tag{10}$$

for some constant z_0 (that depends on U_I) and $\phi(z;c)$ is the travelling-wave solution

$$\frac{d^2\phi}{dz^2} + c\frac{d\phi}{dz} + \phi(1-\phi) = 0, \tag{11}$$
$$\text{as } z \to -\infty \quad \phi \to 1, \text{ as } z \to +\infty \quad \phi \to 0.$$

In view of the z-translation invariance of (11), it is convenient to specify ϕ uniquely via

$$\phi(z;c) \sim 1 - \exp\left(\frac{1}{2}(\sqrt{c^2+4} - c)z\right) \text{ as } z \to -\infty, \tag{12}$$

since (11) can then be solved as an initial-value problem from $z = -\infty$, the condition as $z \to +\infty$ being automatically satisfied for $c > 0$; (11) can readily be, and is traditionally, analysed by phase-plane methods. The appearance of the arbitrary constant z_0 in (10), which depends on the initial data, arises from this translation invariance. For $c = 2$ we have

$$\phi(z;2) \sim Kze^{-z} \quad \text{as } z \to +\infty, \tag{13}$$

corresponding to a degenerate node in the phase plane, where the positive constant K is determined by (11)-(12); for $c > 2$ we instead have

$$\phi(z;c) \sim k(c)\exp(-\frac{1}{2}(c-\sqrt{c^2-4})z) \quad \text{as } z \to +\infty, \tag{14}$$

where $k(c)$ is also determined by (11)-(12), so that

$$k(c) \sim \frac{K}{2(c-2)^{\frac{1}{2}}} \quad \text{as} \quad c \to 2^+.$$

The IVP-character of (11)-(12) motivates us henceforth to adopt

$$u(s(t;\varepsilon),t) = \phi(0;\dot{s}/\Psi^{\frac{1}{2}}(s))\Phi(s) \tag{15}$$

as our definition of s in place of (5); the reason for setting $c = \dot{s}/\Psi^{\frac{1}{2}}(s)$ here will become apparent in Section 3.2.

For the purposes of the subsequent analysis, it is valuable to revisit the reasons for the appearance of the $\ln T$ term in (10). The travelling wave (9) describes the behaviour of (8) as $T \to +\infty$ with $z = O(1)$, but there are two further regions ahead of the wavefront. For $X = O(T)$ we apply the Liouville-Green (JWKB) method (which will be a key ingredient of the analysis throughout this paper) in the form

$$u_0 \sim \ A(X,T)\ e^{-f(X,T)} \tag{16}$$

to obtain (since u_0 is exponentially small for $X/T > 2$)

$$\frac{\partial f}{\partial T} + \left(\frac{\partial f}{\partial X}\right)^2 + 1 = 0, \ \frac{\partial A}{\partial T} + 2\frac{\partial f}{\partial X}\ \frac{\partial A}{\partial X} = -\frac{\partial^2 f}{\partial X^2}A \tag{17}$$

with $f = TF(\eta),\ \eta = X/T$, so that $F(\eta)$ satisfies the Clairaut equation

$$F - \eta\frac{dF}{d\eta} + \left(\frac{dF}{d\eta}\right)^2 + 1 = 0 \tag{18}$$

and hence (since the envelope solution to (18) is the one that we require for fast-decaying initial data)

$$f = \frac{X^2}{4T} - T, \ A = \frac{1}{T^{\frac{1}{2}}}a\left(\frac{X}{T}\right) \tag{19}$$

where a is an arbitrary function that depends on the initial data. The characteristic projections to (17) associated with (19) (i.e. the solutions to the ray equations for (17) in the special case of (17) in which the solutions take the form (19)) each have η constant, i.e. they comprise the expansion fan whereby

$$X/T = \text{constant} \tag{20}$$

holds on each ray. We note that if the initial data are not compactly supported (but decay much more rapidly that $\exp(-X)$ as $X \to +\infty$) there may be a further contribution to the large-time behaviour of the type (16) associated with the initial data but that (19) will be the largest exponential contribution sufficiently close to the wavefront (an example of the exchange of dominance between such contributions is described in [2]). The second additional region is more important (determining as it does the $\ln T$ term in (10) in the current context) and is given by $X = S(T) +$

$O(T^{\frac{1}{2}})$, where $S(T) \sim 2T$ as $T \to +\infty$. In this region we in the first instance set[5]

$$X = S(T) + z, \ u_0 = e^{-z} v,$$

with $z \gg 1$, to give

$$\frac{\partial v}{\partial T} \sim \frac{\partial^2 v}{\partial z^2} + (\dot{S} - 2)\frac{\partial v}{\partial z} - (\dot{S} - 2)v \tag{21}$$

with the matching condition

$$v \sim Kz \quad \text{for} \quad 1 \ll z \ll T^{\frac{1}{2}} \tag{22}$$

following from (13). We then set

$$v = e^{\frac{1}{2}(\dot{S}-2)z} \ e^{-(S-2T)} w \tag{23}$$

to give

$$\frac{\partial w}{\partial T} - \frac{1}{2}\ddot{S} z w \sim \frac{\partial^2 w}{\partial z^2} + \frac{1}{4}(\dot{S} - 2)^2 w. \tag{24}$$

As will follow from (26) below, and as has already in effect been postulated in (10), the second and fourth terms in (24) scale respectively as $w/T^{\frac{3}{2}}$ and w/T^2 as $T \to +\infty$ with $z = O(T^{\frac{1}{2}})$, so prove negligible. Thus we require the large-time solution to

$$\begin{aligned} &\frac{\partial w}{\partial T} = \frac{\partial^2 w}{\partial z^2}, \\ &\text{at } z = 0 \quad w = 0, \end{aligned} \tag{25}$$

where the boundary condition follows from the matching condition (22) on the understanding that (25) pertains to $z = O(T^{\frac{1}{2}})$. Thus (again for fast decay as $z \to +\infty$) we have the usual dipole solution

$$w \sim I_1 \frac{z}{T^{\frac{3}{2}}} \ e^{-z^2/4T} \text{ as } T \to +\infty \text{ with } \ z = O(T^{\frac{1}{2}}),$$

where the positive constant I_1 depends on the initial data, and hence from (22), (23)

$$K \sim e^{-(S-2T)} I_1 \ / T^{\frac{3}{2}},$$

so that

$$S(T) \sim 2T \ - \frac{3}{2}\ln T + \ln(I_1/K) \text{ as } T \to +\infty. \tag{26}$$

We therefore recover (10) with $z_0 = \ln(K/I_1)$ and can deduce that $a(\eta) \sim I_1(\eta - 2)$ as $\eta \to 2^+$.

[5]The procedure we adopt here is not in fact the most transparent one in the current context but is expedient in setting up the framework appropriate to the more involved problems discussed later.

2.2. $\boldsymbol{t = O(\varepsilon^{\frac{1}{3}})}$**.** The second timescale provides the main rationale for the current section: on this timescale two types of universal (parameter-free) large-time behaviours arise, depending on whether λ is positive or negative – these provide concise representations of the distinct types of behaviour that occur for $\Psi^{'}(x) > 0$ and $\Psi^{'}(x) < 0$ and contain many of the essential ingredients of the more general analysis that applies for $t = O(1)$. It is convenient to introduce $\delta = \varepsilon^{1/3}$ and the relevant scalings then read

$$t = \delta\tau, \;\; x = \delta\xi, \;\; s(t;\varepsilon) = \delta\sigma(\tau;\delta). \tag{27}$$

We require

$$\sigma \;\sim\; 2\tau + \delta\sigma_1(\tau) + \delta^2\ln(1/\delta)\sigma_2(\tau) + \delta^2\sigma_3(\tau) \quad \text{as } \delta \to 0. \tag{28}$$

with

$$\sigma_1 \to 0, \;\; \sigma_2 \to -3, \;\; \sigma_3 \sim -\frac{3}{2}\ln\tau - z_0 \quad \text{as } \tau \to 0^+ \tag{29}$$

in order to match with (26). Further, we set

$$\xi = \sigma(\tau;\delta) + \delta\zeta, \quad u = \frac{e^{-\zeta/\delta}}{\delta}v \tag{30}$$

to give for $\zeta > 0$ (so that u is exponentially small) on using (7) that

$$\delta^2\frac{\partial v}{\partial\tau} \sim \delta^2\frac{\partial^2 v}{\partial\zeta^2} + \delta(\dot\sigma - 2)\frac{\partial v}{\partial\zeta} - (\dot\sigma - 2 - \delta\lambda\sigma - \delta^2\mu\sigma^2 - \delta^2\lambda\zeta)v \tag{31}$$

(cf. (21)). Using (28), we immediately obtain from (31) that

$$\dot\sigma_1 = 2\lambda\tau, \quad \dot\sigma_2 = 0$$

at $O(\delta)$ and $O(\delta^2\ln(1/\delta))$ respectively, so, in view of (29),

$$\sigma_1 = \lambda\tau^2, \quad \sigma_2 = -3. \tag{32}$$

At $O(\delta^2)$ we then obtain from (31) the initial-boundary-value problem

$$\begin{aligned} &\frac{\partial v_0}{\partial\tau} = \frac{\partial^2 v_0}{\partial\zeta^2} + 2\lambda\tau\frac{\partial v_0}{\partial\zeta} + \left((\lambda^2 + 4\mu)\tau^2 - \dot\sigma_3 + \lambda\zeta\right)v_0, \\ &\text{at } \zeta \to 0^+ \quad v_0 \sim K\zeta, \\ &\text{as } \tau \to 0^+ \quad v_0 \sim K\zeta\, e^{-\zeta^2/4\tau} \quad \text{for } \zeta = O(\tau^{1/2}); \end{aligned} \tag{33}$$

because a 'known' constant K appears in the boundary data, (33) serves to determine $\sigma_3(\tau)$ as well as $v_0(\zeta,\tau)$. The formulation (33) can be simplified somewhat by setting

$$v_0 = \exp(-\lambda\tau\zeta + \frac{4}{3}\mu\tau^3 - \sigma_3(\tau))w$$

to give[6]

$$\begin{aligned} &\frac{\partial w}{\partial\tau} = \frac{\partial^2 w}{\partial\zeta^2} + 2\lambda\zeta w, \\ &\text{at } \zeta = 0 \quad w = 0, \\ &\text{as } \tau \to 0^+ \quad w \sim \frac{I_1}{\tau^{\frac{3}{2}}}\zeta e^{-\zeta^2/4\tau}, \end{aligned} \tag{34}$$

[6]While the PDE in (34) can readily be mapped to the heat equation (see below), the IBVP is then no longer posed on a fixed domain, so we do not implement the further change of variables here.

with $\sigma_3(\tau)$ then being given in terms of the solution to (34) by

$$\sigma_3 = \frac{4}{3}\mu\tau^3 + \ln\left(\frac{\partial w}{\partial \zeta}(0,\tau)/K\right). \tag{35}$$

The full IBVP (34) governs the wavefront behaviour for $\tau = O(1)$ and we restrict ourselves to determining its large-τ behaviour. The Liouville-Green approach is particularly instructive here: setting

$$w \sim A(\zeta,\tau)e^{-f(\zeta,\tau)}$$

gives

$$\frac{\partial f}{\partial \tau} + \left(\frac{\partial f}{\partial \zeta}\right)^2 + 2\lambda\zeta = 0; \tag{36}$$

this, on introducing $p \equiv \partial f/\partial\zeta,\ q \equiv \partial f/\partial\tau$, implies the ray (Charpit) equations

$$\frac{d\zeta}{d\tau} = 2p,\ \frac{dp}{d\tau} = -2\lambda,\ \frac{df}{d\tau} = q + 2p^2,\ \frac{dq}{d\tau} = 0 \tag{37}$$

(as usual, the ray approach reduces the PDE, here (36), to ODEs, here (37), that govern each of the rays, explicitly reflecting the information flow associated with the first-order (and hence hyperbolic) PDE; the notation in (37) thereby corresponds to expressing the solution to (36) in the form

$$\zeta = \zeta(\tau;p_0),\ f = f(\tau;p_0),\ p = p(\tau;p_0),\ q = q(\tau;p_0),$$

where p_0 in (38) distinguishes distinct rays (i.e. is constant on each ray) and τ parametrises each ray, as described by (37)) subject to the expansion-fan initial data

$$\text{at } \tau = 0 \quad \zeta = 0, \quad f = 0, \quad p = p_0, \quad q = -p_0^2 \tag{38}$$

for arbitrary $p_0 \geq 0$ (i.e. we require the solution to (36) associated entirely with rays that start at $\zeta = 0, \tau = 0$ (in effect because we are interested in the large-time behaviour for localised initial data); similar comments apply for (57)-(58) below). On eliminating p_0, the resulting solution is thus

$$f = \frac{\zeta^2}{4\tau} - \lambda\zeta\tau - \frac{1}{3}\lambda^2\tau^3, \tag{39}$$

the characteristic projections being given by

$$\zeta = 2(p_0\tau - \lambda\tau^2),\ p_0 \geq 0. \tag{40}$$

For $\lambda = 0$ the initial data in (34) of course describe the solution for all τ and, correspondingly, (39)-(40) reduce to

$$f = \frac{\zeta^2}{4\tau}, \quad \zeta = 2p_0\tau$$

(cf. (19)-(20)): this represents a borderline case and the behaviour for $\lambda \neq 0$ is strongly dependent on the sign of λ, as follows.

For $\lambda > 0$ it follows from (40) that the rays turn back on themselves but occupy the whole of $\zeta \geq 0$ for all τ; f is minimal at

$$p_0 = 2\lambda\tau,\ \zeta = 2\lambda\tau^2,\ \text{where } f = -4\lambda^2\tau^3/3,$$

and, more importantly, $\zeta = 0$ corresponds to $p_0 = \lambda\tau$ and $f = -\lambda^2\tau^3/3$ so by (35) we at once obtain

$$\sigma_3 \sim \frac{1}{3}(4\mu + \lambda^2)\tau^3 \quad \text{as } \tau \to +\infty. \tag{41}$$

For $\lambda < 0$, however, the expansion-fan rays (40) occupy only the region $\zeta \geq -2\lambda\tau^2$ and a further family of rays, emanating from $\zeta = 0$ for $\tau > 0$, is required to complete the picture: to characterise these we must first analyse (34) for large τ in the boundary layer $\zeta = O(1)$ (as will be clear from (39), the scaling on which the Liouville-Green solution applies is $\zeta = O(\tau^2)$); here we set

$$w \sim e^{-\nu\tau} W(\zeta) \quad \text{as } \tau \to +\infty, \tag{42}$$

where ν will be determined as an eigenvalue (and (42) can be viewed as being associated with a $\nu\tau$ contribution to f), so that

$$\begin{aligned} &\frac{d^2W}{d\zeta^2} + (2\lambda\zeta + \nu)W = 0, \\ &\text{at} \quad \zeta = 0 \quad W = 0, \\ &\text{as} \quad \zeta \to +\infty \quad \ln W \sim -\frac{2}{3}(-2\lambda)^{1/2}\zeta^{3/2}, \end{aligned} \tag{43}$$

requiring $\lambda < 0$. Thus the solution can be expressed in terms of the Airy function Ai by

$$W = C\ Ai\left((-2\lambda)^{\frac{1}{3}}\zeta - \frac{\nu}{(-2\lambda)^{\frac{2}{3}}}\right), \tag{44}$$

where C is a positive constant that can be expressed in terms of I_1 using the conservation law

$$\frac{d}{d\tau}\int_0^\infty e^{\nu\tau} Ai\left((-2\lambda)^{\frac{1}{3}}\zeta - \frac{\nu}{(-2\lambda)^{\frac{2}{3}}}\right) w(\zeta,\tau)d\zeta = 0$$

and ν is given by

$$\nu = -(-2\lambda)^{\frac{2}{3}} a_0 \tag{45}$$

where $a_0 < 0$ is the first zero of the Airy function,

$$Ai(a_0) = 0. \tag{46}$$

In view of (35), we have

$$\sigma_3 \sim \frac{4}{3}\mu\tau^3 + (-2\lambda)^{\frac{2}{3}} a_0 \tau \quad \text{as } \tau \to +\infty \tag{47}$$

for $\lambda < 0$ (contrast (41)). It follows from matching to (42) that the aforementioned additional ray family for (37) satisfies

$$\text{at } \tau = \tau_0 \quad \zeta = 0,\ f = 0,\ p = 0,\ q = 0 \tag{48}$$

for arbitrary $\tau_0 > 0$ (more precisely, for $\tau_0 \gg 1$ since we are concerned with the large-time behaviour) – in formulating (48), it needs to be observed that the $\nu\tau$ contribution to f implicit in (42) is negligible compared to the solution (49) below that results from (48) on the relevant length scale $\zeta = O(\tau^2)$. Hence

$$f = \frac{2}{3}(-2\lambda)^{\frac{1}{2}}\zeta^{\frac{3}{2}} \tag{49}$$

and the rays are given by

$$\zeta = (-2\lambda)(\tau - \tau_0)^2. \tag{50}$$

In consequence, (39) holds in $\zeta > (-2\lambda)\tau^2$ and (49) in $0 < \zeta < (-2\lambda)\tau^2$ and each satisfies $f = 2(-2\lambda)^2\tau^3/3$, $p = (-2\lambda)\tau$ on $\zeta = (-2\lambda)\tau^2$. The transition between the two can be characterised in more detail by setting

$$\zeta = (-2\lambda)\tau^2 + \hat{\zeta}, \quad w = \exp\left(-\frac{2}{3}(-2\lambda)^2\tau^3 - (-2\lambda)\hat{\zeta}\tau\right)\hat{w}$$

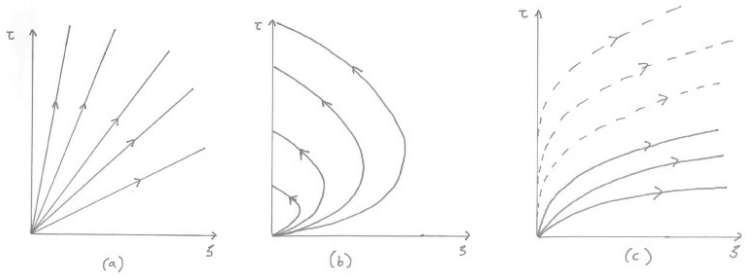

FIGURE 1. Characteristic projections for the eikonal equation (36): (a) $\lambda = 0$, (b) $\lambda > 0$, (c) $\lambda < 0$. The small-τ behaviour of (b) and (c) is as shown in (a), corresponding to the analysis for $\tau = O(1)$. Solid lines: expansion-fan solutions. Dashed lines: rays (50) for $\tau_0 > 0$.

to give from (34) the heat equation

$$\frac{\partial \hat{w}}{\partial \tau} = \frac{\partial^2 \hat{w}}{\partial \hat{\zeta}^2},$$

so that as $\tau \to +\infty$ with $\hat{\zeta} = O(\tau)$ we have

$$\hat{w} \sim \frac{1}{\tau^{1/2}} \Omega\left(\frac{\hat{\zeta}}{\tau}\right) e^{-\hat{\zeta}^2/4\tau}$$

where Ω is an arbitrary function that depends on the initial data but whose far-field behaviour as $\hat{\zeta}/\tau \to \pm\infty$ could in principle be determined from the solutions to the amplitude equation that correspond to (39) and (49).

Important lessons for the analysis that follows can be drawn from the above results. Specifically, for $\lambda > 0$ the front location (as determined from σ_3 in (41)) follows directly from the expansion-fan solution to the Hamilton-Jacobi equation (36) (cf. Section 3.3), whereas a simple manifestation of the differences in behaviour that occur $\lambda < 0$ is that the leading-order contribution in (47) is independent of λ, for reasons clarified in Section 3.2. This distinction results from the very different ray pictures for the large-τ behaviour of (34) shown schematically in Figure 1; note that the dashed rays all emerge tangentially from the τ axis.

3. Analysis for $t = O(1)$.

3.1. **Preamble.** The current section provides the core results of the paper. We start in Sections 3.2 and Sections 3.3 by setting up two plausible mechanisms by which the wavespeed could be selected, both of which give the correct result for pulled fronts when $\Psi(x) \equiv 1$, but which more generally yield distinct results. In the subsequent sub-sections we seek to clarify the reasons why the first is applicable when $\Psi' < 0$ and the second when $\Psi' > 0$. Both approaches rely on linearisation, the first of the travelling-wave ODE and the second of the time-dependent PDE.

3.2. **The repeated-root selection mechanism.** This mechanism is that which arises on requiring the leading-order wavefront location $s_0(t)$ to be that for which the linearisation about $u = 0$ (i.e. as $z \to +\infty$) of the resulting travelling-wave ODE (11) leads to a repeated-root condition on the auxiliary equation for the associated

exponentials, as in (13) (i.e. to a degenerate node in the phase plane). We transform to a travelling-wave frame of reference by setting

$$x = s(t;\varepsilon) + \varepsilon\Psi^{-1/2}(s(t;\varepsilon))z, \quad u = \Phi(s(t;\varepsilon))\tilde{\phi}(z,t) \tag{51}$$

to give

$$\frac{\varepsilon}{\Phi(s)}\left(\frac{\partial\tilde{\phi}}{\partial t} + \dot{s}\left(\frac{1}{2}\frac{\Psi'(s)}{\Psi(s)}z\frac{\partial\tilde{\phi}}{\partial z} + \frac{\Phi'(s)}{\Phi(s)}\tilde{\phi}\right)\right)$$
$$= \frac{\partial^2\tilde{\phi}}{\partial z^2} + \tilde{c}\frac{\partial\tilde{\phi}}{\partial z} + \frac{\Psi(s+\varepsilon\Psi^{-1/2}(s)z)}{\Psi(s)}\tilde{\phi}\left(1 - \frac{\Phi(s+\varepsilon\Psi^{-1/2}(s)z)}{\Phi(s)}\tilde{\phi}\right)$$

where $\tilde{c}(t;\varepsilon) \equiv \dot{s}/\Psi^{1/2}(s)$. Thus setting $\tilde{\phi} \sim \phi(z;c), \tilde{c} \sim c$ as $\varepsilon \to 0$ we recover (11)-(12) at leading order[7]. Linearising (11) about $\phi = 0$ leads to solutions of the form

$$\exp\left(-\frac{1}{2}(c \pm \sqrt{c^2-4})z\right) \tag{52}$$

so the repeated-root (critical-damping/fastest-decay/degenerate-node) condition on solutions to the travelling-wave ODE is simply $c = 2$, i.e.

$$\dot{s}_0 = 2\Psi^{\frac{1}{2}}(s_0), \tag{53}$$

where $s_0(t) = s(t;0)$; moreover, existence of a non-negative wave profile demands (on the basis of the usual phase-plane analysis of (11)) that

$$\dot{s}_0 \geq 2\Psi^{\frac{1}{2}}(s_0).$$

The result (53) represents one of the two selection mechanisms that can pertain and we explore in Section 3.4 the circumstances under which it does in fact apply. Here we simply characterise the behaviour as $t \to 0^+$, with $s_0(0) = 0$ being the leading-order matching condition arising from the previous section. Hence with (7) it is straightforward to obtain the small-time expansion

$$s_0(t) \sim 2t + \lambda t^2 + \frac{4}{3}\mu t^3 \quad \text{as } t \to 0^+, \tag{54}$$

matching successfully with (28) and (32) when (47) holds, but not when (41) does, i.e. (54) is consistent with the results of Section 2 for $\lambda < 0$ but not for $\lambda > 0$.

3.3. **The Hamilton-Jacobi selection mechanism.** Applying the Liouville-Green approach

$$\ln u \sim -f(x,t)/\varepsilon \tag{55}$$

to the linearisation of the PDE (2) yields the eikonal equation

$$\frac{\partial f}{\partial t} + \left(\frac{\partial f}{\partial x}\right)^2 + \Psi(x) = 0 \tag{56}$$

[7]In many formal treatments of slowly varying heterogeneities in other contexts such an analysis (whereby the heterogeneities are in effect frozen at the current front location $x = s$) would suffice to determine the solution. A crucial feature of the current problem is that (11) has a continuum of non-negative solutions (for $c \geq 2$), so the required solution is not yet specified.

with the characteristic equations[8] (involving $p \equiv \partial f/dx,\ q \equiv \partial f/\partial t$)

$$\frac{dx}{dt} = 2p,\ \frac{dp}{dt} = -\Psi^{'}(x),\ \frac{df}{dt} = q + 2p^2,\ \frac{dq}{dt} = 0, \tag{57}$$

for which we are again most interested in the expansion-fan solution, whereby

$$\text{at } t = 0 \quad x = 0,\ p = p_0,\ f = 0,\ q = -p_0^2 - 1 \tag{58}$$

for arbitrary $p_0 \geq 0$. Thus

$$p^2 = p_0^2 + 1 - \Psi(x) \tag{59}$$

holds on rays and, assuming $p > 0$, the solution can be written parametrically in terms of p_0 in the form

$$\int_0^x \frac{dx^{'}}{(p_0^2 + 1 - \Psi(x^{'}))^{\frac{1}{2}}} = 2t, \quad f = \frac{1}{2}\int_0^x \frac{p_0^2 + 1 - 2\Psi(x^{'})}{(p_0^2 + 1 - \Psi(x^{'}))^{\frac{1}{2}}} dx^{'}. \tag{60}$$

Our second putative selection mechanism identifies $s_0(t)$ with the level set $f(s_0(t), t) = 0$ of (56), since this locates the transition between the regimes $x > s_0(t)$ in which u as given by (55) is exponentially small and $x < s_0(t)$ in which $u = O(1)$ and linearisation about $u = 0$ is accordingly inapplicable. Under this scenario $s_0(t)$ is given by the pair of equations

$$\int_0^{s_0(t)} \frac{dx^{'}}{(P_0^2(t) + 1 - \Psi(x^{'}))^{\frac{1}{2}}} = 2t, \quad \int_0^{s_0(t)} \frac{P_0^2(t) + 1 - 2\Psi(x^{'})}{(P_0^2(t) + 1 - \Psi(x^{'}))^{\frac{1}{2}}} dx^{'} = 0 \tag{61}$$

for $s_0(t)$ and $P_0(t)$, the latter variable corresponding to the value of p_0 that instantaneously holds at $x = s_0(t)$ at time t.

The most striking immediate contrast between our two selection criteria (53) and (61) (which we emphasise give different results for $s_0(t)$) is that the former can be viewed as local, while the latter is non-local, in effect requiring the solution of the Hamilton-Jacobi equation (56) for all (x, t). The expressions in (61) can be combined to yield

$$\int_0^{s_0(t)} \left(P_0^2(t) + 1 - \Psi(x^{'})\right)^{\frac{1}{2}} dx^{'} = \left(P_0^2(t) + 1\right) t \tag{62}$$

the time derivative of which yields (on further application of the first of (61))

$$\left(P_0^2(t) + 1 - \Psi(s_0)\right)^{\frac{1}{2}} \dot{s}_0 = P_0^2(t) + 1$$

i.e.

$$P(t)\dot{s}_0 = P^2(t) + \Psi(s_0) \tag{63}$$

where $p = P(t)$ at $x = s_0(t)$; the result (63) also follows immediately by applying (56) to the time derivative of $f(s_0(t), t) = 0$. Hence

$$P(t) = \frac{1}{2}\left(\dot{s}_0(t) - \left(\dot{s}_0^2(t) - 4\Psi(s_0)\right)^{\frac{1}{2}}\right); \tag{64}$$

the negative square root is needed here since then

$$\frac{dx}{dt} = \dot{s_0} - \left(\dot{s}_0^2 - 4\Psi(s_0)\right)^{\frac{1}{2}} < \dot{s}_0 \quad \text{at} \quad x = s_0$$

[8]It is instructive to compare (57) with the characteristic equations for the inhomogeneous Helmholtz equation, say: considerable insight into the current problem follows by technology transfer from classical treatments of linear-wave propagation; we emphasise, though, that the results here have direct implications for genuinely nonlinear phenomena.

i.e. the ray is moving at a slower speed than the front $x = s_0(t)$ and hence enters, rather than emerging from, it; this choice of square root is also needed to match back into the leading edge of the travelling wave (cf. (14)). It can at once again be inferred that

$$\dot{s}_0 \geq 2\Psi^{\frac{1}{2}}(s_0) \tag{65}$$

(compare the result (53) that applies for the other selection mechanism), with equality holding only in exceptional circumstances whenever the Hamilton-Jacobi mechanism applies (see below).

The (non-generic) case $\Psi(x) \equiv 1$ is instructive here: (60)-(61) imply

$$f = \frac{x^2}{4t} - t, \quad s_0(t) = 2t, \quad P_0(t) = 1, \tag{66}$$

so that both (53) and (61) give the same result; because P_0 is constant in (66) the level set $f = 0$ is in this case also a ray of (56) and, exceptionally, can be tracked independently of the solution on the other rays (see [2] for further discussion of such matters).

The small-t behaviour can fairly readily be constructed from the first of (61) and (62), say, giving

$$s_0(t) \sim 2t+\lambda t^2+\frac{1}{3}(4\mu+\lambda^2)t^3,\ P_0(t) \sim 1+\lambda t+\frac{1}{6}(8\mu+\lambda^2)t^2,\ P(t) \sim 1+\frac{1}{6}(\lambda^2-4\mu)t^2 \tag{67}$$

at $t \to 0^+$, so that

$$\dot{s}_0^2 - 4\Psi(s_0) \sim 4\lambda^2 t^2, \dot{s}_0/\Psi^{\frac{1}{2}}(s_0) \sim 2 + \lambda^2 t^2 \quad \text{as} \quad t \to 0^+. \tag{68}$$

The first of (67) is consistent with (41) but not with (47), already hinting at our key conclusion, namely that the repeated-root and Hamilton-Jacobi mechanisms apply respectively to the cases $\Psi^{'}(x) < 0$ and $\Psi^{'}(x) > 0$, with the classical case $\Psi(x) \equiv 1$ corresponding to a non-generic borderline regime in which both simultaneously apply.

3.4. **Applicability of the repeated-root mechanism.** The eikonal equation (56) will be crucial throughout what follows. In this subsection we discuss the behaviour of rays that enter or depart the level set

$$f\,(s_0(t), t) = 0 \tag{69}$$

when s_0 is given by (53). An important criterion here is that, on a given ray, the solution to (57) is not acceptable at time t if

$$f(x, t^{'}) < 0 \quad \text{at any time} \quad t^{'} \in [t_0, t] \tag{70}$$

where $t_0 \geq 0$ is the time at which the ray first emerges: (70) corresponds to exponentially large u, so that the PDE linearisation that leads to (56) is inapplicable. In other words, the nonlinearity serves as a 'self-generating' obstacle through which it is not admissible to propagate the rays.

The relevant ray families satisfy (using (64) with (53))

$$\text{at } t = t_0, \quad x = s_0(t_0), \quad p = \Psi^{\frac{1}{2}}(s_0), \quad f = 0,\ q = -2\Psi(s_0) \tag{71}$$

with $s_0(t)$ given by (53) and where $t > t_0$ holds on rays departing the front and $t < t_0$ on those entering it. Of most significance here is the behaviour close to $t = t_0$; we have from (57) and (71) that

$$\frac{dx}{dt} = 2\Psi^{\frac{1}{2}}(s_0) \text{ at } t = t_0 \tag{72}$$

(we retain the notation d/dt in place of $\dot{}$ in such expressions as a reminder that the derivative is to be taken along a ray) so that the ray is tangential to the front (see (53)), while (53) and (57) imply respectively that

$$\ddot{s}_0 = 2\Psi'(s_0), \quad \frac{d^2x}{dt^2} = -2\Psi'(x). \tag{73}$$

Thus if $\Psi' > 0$ the front would be accelerating and the ray decelerating, and conversely for $\Psi' < 0$; moreover,

$$\frac{df}{dt} = 0, \quad \frac{d^2f}{dt^2} = -4\Psi^{\frac{1}{2}}(s_0)\Psi'(s_0) \quad \text{at } t = t_0 \tag{74}$$

so for $\Psi' > 0$ such a ray lies in $x < s(t_0)$ and has $f < 0$ for $t \neq t_0$: it is thus inadmissible by (70). By contrast, for $\Psi' < 0$ the ray lies in $x < s_0(t)$ and has $f > 0$ for $t \neq t_0$.

As we shall see, various different ray families associated with different $f(x,t)$ are typically present. The one of most significance at any given t is the admissible one that has $f(x,t) = 0$ for the largest value of x (thereby determining $s_0(t)$). The immediate conclusions[9] of the preceding analysis are the following.

(Ia) (53) cannot hold for $\Psi'(x) > 0$ since no admissible $f(x,t)$ is then present immediately ahead of the wavefront. Since (11)-(12) has a non-negative solution only for $c \geq 2$, an immediate implication is that

$$\dot{s}_0 > 2\Psi^{\frac{1}{2}}(s_0) \tag{75}$$

must generically hold for $\Psi'(x) > 0$.

(IIa) For $\Psi'(x) < 0$, however, the result (53) cannot be excluded (and we shall conclude later that it indeed holds). For a ray satisfying (71), the part of the ray having $t < t_0$ is not in general of interest, the initial data having to be of a very specific form to generate such a ray (cf. [2]), but the part with $t > t_0$ (i.e. that emanating from, rather than entering, the front) plays an important role in establishing the complete picture.

3.5. **Applicability of the Hamilton-Jacobi mechanism.** Here we need to revisit the expansion-fan problem (57)-(58), the rays for which all have $t_0 = 0$, and pay particular attention to the rays having p_0 in the neighbourhood of $p_0 = 1$, since the leading-order solution for small t is that which applies for all time when $\Psi(x) \equiv 1$, i.e.

$$f \sim (p_0^2 - 1)t, \quad x \sim 2p_0 t \quad \text{as} \quad t \to 0^+; \tag{76}$$

in view of (70), $p_0 \geq 1$ is thus a necessary condition for a ray to be admissible.

Now (57)-(58) imply, using (59), that

$$\frac{df}{dt} = 2p^2 - p_0^2 - 1 = p_0^2 + 1 - 2\Psi(x), \quad \frac{d^2f}{dt^2} = -4\Psi'(x)p, \tag{77}$$

and for $\Psi'(x) < 0$ we have that p increases monotonically on rays (with $x(t)$ accelerating: see (73)): in consequence all rays having $p_0 \geq 1$ remain admissible for all t but all have $f(x,t) > 0$ for $t > 0$ so cannot play a role in determining $s_0(t)$. However, for $\Psi'(x) > 0$ with $p_0^2 < \Psi_\infty - 1$, where Ψ_∞ is defined by (4), it follows that p will change sign, with $p = 0$ at $t = t^*(p_0)$, say, such that

$$\dot{x} = 2\left(p_0^2 + 1 - \Psi(x)\right)^{\frac{1}{2}}, \quad 0 < t < t^*, \quad \dot{x} = -2\left(p_0^2 + 1 - \Psi(x)\right)^{\frac{1}{2}}, \quad t > t^*.$$

[9] See the next subsection for the 'partner' conclusions (Ib) and (IIb).

Such expansion-fan rays cannot cross while $p > 0$ since for given x their speed increases with p_0; once p drops below zero, however, they can do so (associated in the usual way with shock formation in (99) below), the resulting multivaluedness requiring consideration to be given to which carries the dominant contribution to u. Writing $x = x^*(p_0)$ at $t = t^*$, it follows that x^* is given by

$$\Psi(x^*) = p_0^2 + 1; \tag{78}$$

moreover,

$$x(t) = x(2t^* - t), \quad p(t) = -p(2t^* - t) \tag{79}$$

hold on each of these rays. On rays with $p_0^2 > \Psi_\infty - 1$ we have

$$p \sim (p_0^2 + 1 - \Psi_\infty)^{\frac{1}{2}}, \quad x \sim 2(p_0^2 + 1 - \Psi_\infty)^{\frac{1}{2}} t, \quad f \sim (p_0^2 + 1 - 2\Psi_\infty)t \quad \text{as } t \to +\infty \tag{80}$$

and on those with $p_0^2 < 2\Psi_\infty - 1$ it follows that $f(x,t)$ will first increase and then decrease through zero; on rays with $p_0^2 > 2\Psi_\infty - 1$ we instead have that f, $\dot{f} > 0$ for all t. There are now two subcases to treat when $\Psi'(x) > 0$, as follows.

(A) $1 < \Psi_\infty \leq 2$. Here t^* exists only for rays with $p_0^2 < \Psi_\infty - 1 < 1$, and these (for reasons already noted) are all inadmissible. This is the simplest such case, $s_0(t)$ being determined via (69) through the rays with $1 < p_0^2 < 2\Psi_\infty - 1$, on which $f > 0$ for $x > s_0(t)$ and $f < 0$ for $x < s_0(t)$ (see (76) for the small-t behaviour, giving $s_0 \sim 2t$, and (80) for the large-t, whereby $s_0 \sim 2\Psi_\infty^{\frac{1}{2}} t$). Further insight into the significance of the value $\Psi_\infty = 2$ is provided by the example in Appendix 2.

(B) $\Psi_\infty > 2$. Here the prescription described in (A) will give the behaviour of $s_0(t)$ for sufficiently large t ((80) applying for $p_0^2 > \Psi_\infty - 1$). However, for smaller t (and for all t if Ψ_∞ is unbounded) the wavefront is determined by the rays having $1 < p_0^2 < \Psi_\infty - 1$: on these rays, p changes sign as described above, with f decreasing while $x > x^\dagger$, where $x^\dagger < x^*$ and

$$\Psi(x^\dagger) = (p_0^2 + 1)/2 = \Psi(x^*)/2 \tag{81}$$

determines $x^\dagger(p_0)$; f then increases once x drops below $x^\dagger$ again: on such a ray, $f(t)$ can be written in the form

$$f(t) = F(t) - F(0) \text{ where } F(t) = -F(2t^* - t). \tag{82}$$

Since $F(t^*) = 0$, this is equivalent to

$$f(t) = F(t) + f(t^*),$$

so that

$$F(t) = -\frac{1}{2} \int_x^{x^*} \frac{p_0^2 + 1 - 2\Psi(x')}{(p_0^2 + 1 - \Psi(x'))^{\frac{1}{2}}} dx' \quad \text{for} \quad t < t^*, \tag{83}$$

wherein $x(t)$ is given by the first of (60).

It is straightforward to see that $P(t) > 0$ holds for rays with p_0^2 just greater than 1 or (for finite Ψ_∞) just less than $\Psi_\infty - 1$; indeed, corresponding to former case we have $P_0 \sim P \sim 1$ as $t \to 0^+$. However, for $p_0^2 \in (1, \Psi_\infty - 1)$ but away from these two limits P need not be positive; for the rest of this section we shall, however, assume that it is and return to the matter in Section 4. Under this assumption, tracking the level set $f = 0$ leads to (61) determining $s_0(t)$ with no further complications.

The main conclusions are now:

(Ib) for $\Psi'(x) < 0$ the admissible expansion-fan rays all have $f > 0$ for $t > 0$ and hence cannot determine the front location;

(IIb) for $\Psi'(x) > 0$, the level set $f(x,t) = 0$ of the expansion-fan solution provides

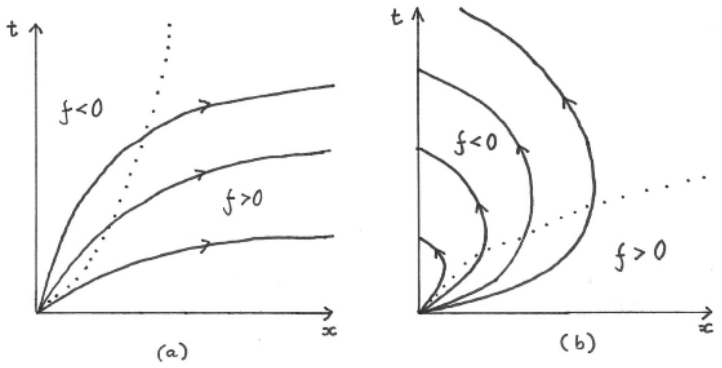

FIGURE 2. Expansion fans for (a) $\Psi'(x) < 0$ and (b) $\Psi'(x) > 0$. Solid lines: rays. Dotted line: level set $f = 0$. Note that the rays in (a) enter $f = 0$ from the inadmissible region $f < 0$.

a plausible front location $x = s_0(t)$ (and does indeed determine it under suitable constraints, described below).

Schematics of the expansion-fan rays clarifying the above remarks are shown in Figure 2. The level set $f = 0$ in Figure 2(a) moves faster than the minimum wavespeed as determined by the repeated-root condition: that the latter applies for $\Psi' < 0$ is associated with the decrease in the net birth rate with increasing u expressed in the nonlinearity in (2) – i.e. the nonlinearity results in a self-limiting wave; thus while the repeated-root condition follows from a linear analysis, the resulting selection mechanism is not intrinsically linear in quite the same way as the Hamilton-Jacobi one. We note that the criteria identified in (Ia)-(Ib) and (IIa)-(IIb) are complementary, i.e. distinct putative mechanisms have now been identified for $\Psi'(x) < 0$ and $\Psi'(x) > 0$; we adduce below further evidence for the validity of this identification.

3.6. **Correction terms.** Given the interest that the logarithmic correction term has garnered in the classical case $\Psi(x) \equiv 1$, i.e. (under the current scalings) the second and third terms in the expansion

$$s(t;\varepsilon) \sim 2t - \frac{3}{2}\varepsilon \ln(1/\varepsilon) - \frac{3}{2}\varepsilon \ln t, \tag{84}$$

we here pursue the corresponding analyses for variable $\Psi(x)$.
(I) $\Psi'(x) < 0$. Taking (53) to hold, the analysis closely follows that of Section 2. We set[10]

$$s(t;\varepsilon) \sim s_0(t) + \varepsilon^{\frac{2}{3}} s_1(t), \quad x = s(t;\varepsilon) + \varepsilon^{\frac{2}{3}}\zeta \tag{85}$$

and

$$u = \frac{e^{-\Psi^{\frac{1}{2}}(s_0)\zeta/\varepsilon^{\frac{1}{3}}}}{\varepsilon^{\frac{1}{3}}} v,$$

[10]It is noteworthy that even the scaling with respect to ε of the correction term in the first of (85) differs from those in (84).

wherein the decay rate of the exponential is that associated with a repeated root, to give

$$\frac{\partial^2 v_0}{\partial \zeta^2} + \left(2\Psi^{'}(s_0)\zeta + \Psi^{'}(s_0)s_1 - \Psi^{\frac{1}{2}}(s_0)\dot{s}_1\right) v_0 = 0, \tag{86}$$

$$\text{as } \zeta \to 0^+ \quad v_0 \sim K\zeta,$$
$$\text{as } \zeta \to +\infty \quad v_0 \to 0.$$

Hence

$$v_0 = K\frac{Ai\left(\left(-2\Psi^{'}(s_0)\right)^{\frac{1}{3}}\zeta + a_0\right)}{\left(-2\Psi^{'}(s_0)\right)^{\frac{1}{3}} Ai^{'}(a_0)} \tag{87}$$

with $s_1(t)$ being determined by

$$\Psi^{\frac{1}{2}}(s_0)\dot{s}_1 - \Psi^{'}(s_0)s_1 = \left(-2\Psi^{'}(s_0)\right)^{\frac{2}{3}} a_0, \tag{88}$$

the complementary function of which has $s_1 \propto \dot{s}_0$, as is to be expected in view of the t-translation invariance of the problem. From (88) we have

$$s_1 \sim (-2\lambda)^{\frac{2}{3}} a_0 t \quad \text{as } t \to 0^+,$$

thereby matching with (45). The appearance of an Airy function in (87) should be no surprise: since the rays depart a repeated-root front (53) tangentially, the latter corresponds to a caustic (cf. a creeping field in the geometrical theory of diffraction).

(II) $\Psi^{'}(x) > 0$. Since the Hamilton-Jacobi mechanism applies in this case, we need to consider the amplitude equation for $A(x,t)$ in the Liouville-Green ansatz

$$u \sim \varepsilon^{\frac{1}{2}} A(x,t) e^{-f(x,t)/\varepsilon} \tag{89}$$

wherein f is given as above and A satisfies

$$\frac{\partial A}{\partial t} + 2\frac{\partial f}{\partial x}\frac{\partial A}{\partial x} = -\frac{\partial^2 f}{\partial x^2} A \tag{90}$$

(cf. (17)) so writing

$$A^2 = \frac{\partial E}{\partial x} \tag{91}$$

gives

$$\frac{\partial E}{\partial t} + 2\frac{\partial f}{\partial x}\frac{\partial E}{\partial x} = 0$$

without loss of generality, so that E is constant on rays of (56), and in view of (57) we may set $E = E(q)$, where E is an arbitrary function. Reconstructing A from (91) and matching with (19), this matching requiring the $\varepsilon^{\frac{1}{2}}$ prefactor in (89), implies

$$A(x,t) = \frac{\left(-\frac{\partial^2 f}{\partial x \partial t}\right)^{\frac{1}{2}}}{\left(-\frac{\partial f}{\partial t} - 1\right)^{\frac{1}{4}}} \quad a\left(2\left(-\frac{\partial f}{\partial t} - 1\right)^{\frac{1}{2}}\right), \tag{92}$$

where a is the same function as in (19), being determined as the large-time far-field of the nonlinear problem (8), so that it depends on the initial data $U_I(X)$ in a manner that is presumably not susceptible to analytical characterisation.

By taking derivatives of (56) with respect to t and x and the first and second derivatives of $f(s_0(t),t)=0$ with respect to t, we find using (63) that

$$\frac{\partial f}{\partial t}=-\dot{s}_0P,\quad \frac{\partial^2 f}{\partial x\partial t}=\frac{2\ddot{s}_0P^2-\dot{s}_0^2\Psi'(s_0)}{\dot{s}_0^2-4\Psi(s_0)}\quad\text{at}\quad x=s_0(t),$$

where $s_0(t)$ is given by (61) and $P(t)$ by (64); equivalent statements that make the signs of these quantities more explicit are

$$\frac{\partial f}{\partial t}=-P_0^2-1,\quad \frac{\partial^2 f}{\partial x\partial t}=-\frac{2P_0\dot{P}_0}{(\dot{s}_0^2-4\Psi(s_0))^{\frac{1}{2}}}\quad\text{at}\quad x=s_0(t),\tag{93}$$

the latter following on using the first derivatives of (63) and of

$$p^2(t)=p_0^2(t)+1-\Psi(s_0).$$

In (93), $\dot{P}_0>0$ follows either by consideration of the relevant rays or by differentiating the first of (61) to give

$$P_0\dot{P}_0\int_0^{s_0}\frac{dx'}{(P_0^2+1-\Psi(x'))^{\frac{3}{2}}}=\frac{\left(\dot{s}_0^2-4\Psi(s_0)\right)^{\frac{1}{2}}}{P}$$

and further such manipulations are possible using the identities (see (63))

$$P_0^2+1=P^2+\Psi(s_0)=\dot{s}_0P.$$

We then find on matching to (14) using (51) that the correction terms to the front location are given by

$$s(t;\varepsilon)\sim s_0(t)-\varepsilon\ln(1/\varepsilon)\frac{1}{2P(t)}+\varepsilon\frac{1}{P(t)}\ln\left(\frac{A(s_0,t)}{k(\dot{s}_0/\Psi^{\frac{1}{2}}(s_0))}\right)\quad\text{as}\quad\varepsilon\to0.\tag{94}$$

Since by (93)

$$A(s_0,t)=\left(\frac{2\dot{P}_0}{(\dot{s}_0^2-4\Psi(s_0))^{\frac{1}{2}}}\right)^{\frac{1}{2}}a(2P_0),$$

we have by (67) and (68) that

$$A(s_0,t)\sim2\lambda I_1t^{\frac{1}{2}}\quad\text{as}\quad t\to0^+,$$

while (68) implies that

$$k(\dot{s}_0/\Psi^{\frac{1}{2}}(s_0))\sim K/2\lambda t\quad\text{as}\quad t\to0^+.$$

Hence $s(t;\varepsilon)$ contains a term $3\varepsilon\ln t/2$ as $t\to0^+$ (we emphasise that this has the opposite sign from that in (84)), implying consistent matching of (94) for $\tau=O(1),t=O(\varepsilon^{\frac{1}{3}})$ with the $-3\delta^2\ln(1/\delta)$ term in (28).

As is implicit in the above analysis, in this case the correction terms to the front location, as expressed by (94), are in effect determined solely by the ray solution, in contrast to (I) above in which a narrow region ahead of the wavefront plays a crucial role.

4. **Initiation of additional fronts for $\Psi'(x) > 0$.** Here we investigate an effect identified by [6] whereby two (or indeed more) additional fronts (one in each pair moving to the right and the other to the left) can be initiated ahead of the original front (and for which analogies can be drawn with quantum tunneling); this behaviour arises when P drops below zero (cf. comments near the end of Section 3.5). In consequence, the position of the leading front appears to be discontinuous, jumping forward to the initiation point of the new fronts; nevertheless, the individual fronts each behave in a continuous fashion.

Two scenarios are possible. In the first, the Hamilton-Jacobi selection mechanism applies throughout the life-times of all three fronts. The new fronts are initiated when there exists an x^* as in (78) for which $f = 0$ as well as $p = 0$ at $x = x^*$ i.e. (by (60) and using (78)) an x^* satisfying

$$\int_0^{x^*} \frac{\Psi(x^*) - 2\Psi(x)}{(\Psi(x^*) - \Psi(x))^{\frac{1}{2}}}\, dx = 0. \tag{95}$$

For $\Psi'(x) > 0$ the left-hand side of (95) is negative for both large and small x^*, so if there is a solution x^* to (95) then there are generically at least two, and (as is already implicit) we focus on the case in which there are exactly two, which we denote by $x^* = x_1$ and $x^* = x_2$ with $x_1 > x_2$, and we write

$$p_1^2 + 1 = \Psi(x_1), \quad p_2^2 + 1 = \Psi(x_2) \tag{96}$$

(see (78)) and, by (60),

$$t_1 = \frac{1}{2}\int_0^{x_1} \frac{dx}{(\Psi(x_1) - \Psi(x))^{\frac{1}{2}}}, \quad t_2 = \frac{1}{2}\int_0^{x_2} \frac{dx}{(\Psi(x_2) - \Psi(x))^{\frac{1}{2}}} \tag{97}$$

with $p_1 > p_2$, $t_2 > t_1$; the latter inequality is implied by the following argument: (95), (97) yield

$$t_1 = \frac{1}{\Psi(x_1)}\int_0^{x_1} (\Psi(x_1) - \Psi(x))^{\frac{1}{2}} dx, \; t_2 = \frac{1}{\Psi(x_2)}\int_0^{x_2} (\Psi(x_2) - \Psi(x))^{\frac{1}{2}} dx, \tag{98}$$

while

$$\int_0^{x} \frac{\Psi(x) - 2\Psi(x')}{(\Psi(x) - \Psi(x'))^{\frac{1}{2}}}\, dx' > 0 \quad \text{for} \quad x_2 < x < x_1;$$

hence

$$\frac{d}{dx}\, \frac{1}{\Psi(x)}\int_0^{x} (\Psi(x) - \Psi(x'))^{\frac{1}{2}} dx' = -\frac{\Psi'(x)}{2\Psi^2(x)}\, \int_0^{x} \frac{\Psi(x) - 2\Psi(x')}{(\Psi(x) - \Psi(x'))^{\frac{1}{2}}}\, dx' < 0$$

for $x_2 < x < x_1$, so $t_1 < t_2$ by (98).

Further insight can obtained by tracking the curves on which $p = 0$, so that x is given in terms of p_0 by (78) but x^* does not in general satisfy (95). Denoting such a curve by $x = \sigma(t)$, it follows from

$$\frac{\partial p}{\partial t} + 2p\frac{\partial p}{\partial x} + \Psi'(x) = 0 \tag{99}$$

that

$$\dot\sigma = \Psi'(\sigma)/\frac{\partial p}{\partial x}(\sigma, t), \tag{100}$$

so that at a minimum with respect to x of f (corresponding to a maximum of u) we have $\dot\sigma > 0$, while $\dot\sigma < 0$ holds at a maximum with respect to x of f. For the

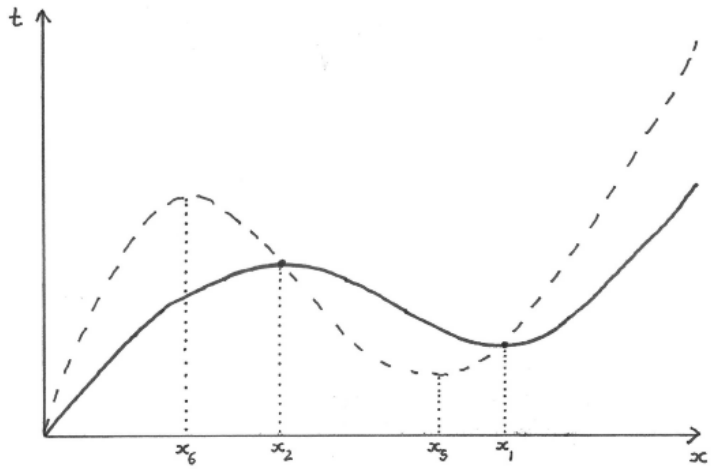

FIGURE 3. The solid curve denotes $x = s_0(t)$ and the dashed one $x = \sigma(t)$ ($p > 0$ holds below the dashed curve and $p < 0$ above it), the rays crossing the latter vertically; $\partial p/\partial x$ is positive on $x = \sigma(t)$ for $0 < x < x_6$ and for $x > x_5$ and is negative in $x_6 < x < x_5$. The borderline case corresponding to (95), (102) has $x_1 = x_2 = x_5$, with $s_0(t)$ monotically increasing but with $\dot{s}_0$ unbounded at $t = t_1 = t_2$.

record, the ray solution given in Section 3.3 can be manipulated to express $\partial p/\partial x$ in the form

$$\frac{\partial p}{\partial x}(x,t) = \frac{1}{p\int_0^x \frac{dx'}{(p_0^2+1-\Psi(x'))^{\frac{3}{2}}}} \left(\frac{1}{p_0} - \frac{1}{2}\int_0^x \frac{\Psi'(x)-\Psi'(x')}{(p_0^2+1-\Psi(x'))^{\frac{3}{2}}}dx\right)$$

so that

$$\frac{\partial p}{\partial x}(\sigma,t) = \frac{\Psi'(\sigma)}{2}\left(\frac{1}{(\Psi(\sigma)-1)^{\frac{1}{2}}} - \frac{1}{2}\int_0^\sigma \frac{\Psi'(\sigma)-\Psi'(x)}{(\Psi(\sigma)-\Psi(x))^{\frac{3}{2}}}dx\right). \tag{101}$$

The borderline case for $\Psi(x)$ in terms of whether or not new fronts are initiated arises when (95) has a repeated root: the resulting condition can be deduced (on taking careful account of the singularity in the integrand at $x = x^*$) in the form

$$\int_0^{x^*} \frac{\Psi'(x^*)-\Psi'(x)}{(\Psi(x^*)-\Psi(x))^{\frac{3}{2}}}dx = \frac{2}{(\Psi(x^*)-1)^{\frac{1}{2}}}; \tag{102}$$

from (101) we see that this corresponds to f having an inflection point at $x = x^*$, as is to be expected. It is readily seen that (101) is positive for both small and large σ and the overall behaviour of $x = \sigma(t)$ and $x = s_0(t)$ in the current regime (in which $s_0(t)$ is multivalued for $t_1 \le t \le t_2$) is illustrated schematically in Figure 3.

Near the point (x_1, t_1) at which the new fronts are initiated, we have

$$f \sim \frac{1}{2}\frac{\partial p}{\partial x}(x_1,t_1)(x-x_1)^2 - \Psi(x_1)(t-t_1),$$

in which $\partial p/\partial x$ is given by (101), so that

$$s_0(t) \sim x_1 \pm \left(\frac{2\Psi(x_1)}{\frac{\partial p}{\partial x}(x_1,t_1)} \right)^{\frac{1}{2}} (t-t_1)^{\frac{1}{2}} \quad \text{as} \quad t \to t_1^+,$$

i.e. both start with unbounded velocity; similarly

$$s_0(t) \sim x_2 \pm \left(\frac{2\Psi(x_2)}{-\frac{\partial p}{\partial x}(x_2,t_2)} \right)^{\frac{1}{2}} (t_2-t)^{\frac{1}{2}} \quad \text{as} \quad t \to t_2^-,$$

illustrating how then new leftward moving front collides with the original rightward moving one at $t = t_2$, leading to their mutual annihilation (associated with which there will be a short timescale (as there is for t close to t_1) in which a different balance pertains in (2) – we shall not discuss such matters here). The ray solution in Section 3.3 treats the case in which only the positive square root is required when extracting p from (58); here we also need the negative one in determining the location of the leftward moving front with $x_2 < s_0(t) < x_1$ (both rightward moving ones are given by (61)). The symmetry results of Section 3.5 readily provide the relevant prescription in the form

$$\begin{aligned} &\int_0^{s_0(t)} \frac{dx'}{(P_0^2(t)+1-\Psi(x'))^{\frac{1}{2}}} + 2\int_{s_0(t)}^{\Sigma(t)} \frac{dx'}{(P_0^2(t)+1-\Psi(x'))^{\frac{1}{2}}} = 2t, \\ &\int_0^{s_0(t)} \frac{P_0^2(t)+1-2\Psi(x')}{(P_0^2(t)+1-\Psi(x'))^{\frac{1}{2}}} dx' + 2\int_{s_0(t)}^{\Sigma(t)} \frac{P_0^2(t)+1-2\Psi(x')}{(P_0^2(t)+1-\Psi(x'))^{\frac{1}{2}}} dx' = 0, \end{aligned} \tag{103}$$

which, along with $\Psi(\Sigma) = P_0^2 + 1$, determine $s_0(t), P_0(t)$ and $\Sigma(t), x = \Sigma$ giving the location at which the ray having the associated value of P_0 changes direction. $P(t)$ takes the opposite sign from before, i.e. (63)-(64) become

$$-P(t)\dot{s}_0 = P^2(t) + \Psi(s_0), \;\; P(t) = -\frac{1}{2}\left(\dot{s}_0(t) - \left(\dot{s}_0^2(t) - 4\Psi(s_0) \right)^{\frac{1}{2}} \right). \tag{104}$$

The above assumes that the level set $f(s_0(t),t) = 0$ spans the full range $x_2 < x < x_1$, but this need not be the case, the second scenario alluded to above occurring when f fails to drop below zero on some of the relevant rays; roughly speaking, the sequence followed as $\Psi(x)$ increases over narrower and narrower regions is that of Section 3, then the first scenario above and finally the one that we now address. On rays with $p_0^2 < \Psi_\infty - 1$ we have that x increases to $x = x^*$ (as in (78)) and then decreases again, as described by (79). The locations x_1 and x_2 are defined as above, but there are now additional points $(x_3,t_3),(x_4,t_4)$ with $x_1 > x_3 > x_4 > x_2, t_1 < t_3 < t_4 < t_2$ that require consideration: at x_3 and x_4, p_0 is related to x by (81), so that df/dt is zero there, and t_3 and t_4 denote the second time that the ray in question has visited x_3 and x_4, respectively; these points are identified by the criterion that $f = 0$ also holds there, this being the minimum value of f attained on the corresponding rays. While the ray solution (60) holds only for $t < t^*$, the symmetry conditions such as (82) enable us to determine x_3 and x_4 as solutions $x^\dagger$ to

$$\int_0^{x^\dagger} \frac{\Psi(x^\dagger)-\Psi(x)}{(2\Psi(x^\dagger)-\Psi(x))^{\frac{1}{2}}} dx + 2\int_{x^\dagger}^{x^*} \frac{\Psi(x^\dagger)-\Psi(x)}{(2\Psi(x^\dagger)-\Psi(x))^{\frac{1}{2}}} dx = 0, \tag{105}$$

wherein x^* is given by $\Psi(x^*) = 2\Psi(x^\dagger)$; the first integral in (105) is positive and the second negative.

Since $P_0^2 + 1 = 2\Psi(s_0), P = -\Psi^{\frac{1}{2}}(s_0)$ at $x = x_3, x_4$ we have by (104) that

$$\dot{s}_0 = -2\Psi^{\frac{1}{2}}(s_0) \tag{106}$$

at $t = t_3, t_4$ and the ray is tangential to the front, providing the clue that the leftward moving front initially propagates for $t > t_3$ according to the repeated-root condition (no Hamilton-Jacobi selection mechanism being available), i.e. according to (106) (since x is decreasing, it is propagating in the direction of decreasing Ψ, so this scenario is consistent with the analysis of Section 3). The remaining question concerns where and how the Hamilton-Jacobi mechanism reasserts itself as s_0 decreases. To investigate this, it is convenient to introduce $x = \omega(t)$ as the zero level set of df/dt on rays, since this passes through both (x_3, t_3) and (x_3, t_4). The ray solution yields that $\omega(t)$ is given by

$$2\int_0^\sigma \frac{dx}{(\Psi(\sigma) - \Psi(x))^{\frac{1}{2}}} - \int_0^\omega \frac{dx}{(\Psi(\sigma) - \Psi(x))^{\frac{1}{2}}} = 2t,$$

where $\Psi(\sigma) = 2\Psi(\omega) = p_0^2 + 1$, i.e. $\sigma(t)$ is defined in the same way as above and, since

$$\Psi'(\sigma)\dot{\sigma} = 2\Psi'(\omega)\dot{\omega}$$

and we are concerned with the range in which $\partial p/\partial x < 0$ (cf. Figure 3), it follows from (100) that $\dot{\omega} < 0$. Since $p = -\Psi^{\frac{1}{2}}(\omega), q = -2\Psi(\omega)$ on the relevant part of $x = \omega$ we have

$$\frac{d}{dt} f(\omega(t), t) = -2\Psi(\omega) - \Psi^{\frac{1}{2}}(\omega)\dot{\omega} \tag{107}$$

so that, using the definitions $f(x_3, t_3) = f(x_4, t_4) = 0, f(\omega(t), t) > 0$ for $t_3 < t < t_4$, we obtain

$$\int_{x_3}^{\Sigma} \frac{dx}{2\Psi^{\frac{1}{2}}(x)} + t - t_3 = -\frac{f(\omega, t)}{2\Psi(\omega)} - \frac{1}{2}\int_{t_3}^{t} \frac{f(\omega(t'), t')\Psi'(\omega(t'))\dot{\omega}(t')}{\Psi^2(\omega(t'))} dt',$$

and hence

$$\int_{x_3}^{x_4} \frac{dx}{2\Psi'(x)} + t_4 - t_3 = -\frac{1}{2}\int_{t_3}^{t_4} \frac{f(\omega(t'), t')\Psi'(\omega(t'))\dot{\omega}(t')}{\Psi^2(\omega(t'))} dt'. \tag{108}$$

Since

$$\int_{x_3}^{s_0(t)} \frac{dx}{2\Psi^{\frac{1}{2}}(x)} + t - t_3 = 0 \tag{109}$$

it follows from (108)-(109), wherein $f, \Psi' > 0$ and $\dot{\omega} < 0$, that $s_0(t_4) < x_4$ and the front behaviour is as indicated in Figure 4; there will again be a fast transient timescale over which two of the fronts annihilate, which will occur at some point x_7 with $x_7 < x_4$ but where $x_2 - x_7$ can presumably take either sign.

It is clear the above behaviour can be repeated arbitrarily often (for example by considering $\Psi(x)$ that see rapid growth about a number of highly disparate values of x), with a sequence new fronts arising and being annihilated. It is possible, however, for such potential additional fronts to be overrun before they get the chance to form. Determining the correction terms for the locations of new fronts would be awkward. For the power-law case discussed in [2], a related phenomenon occurs for $n \geq 2$ whereby a new front is initiated at $x = +\infty$.

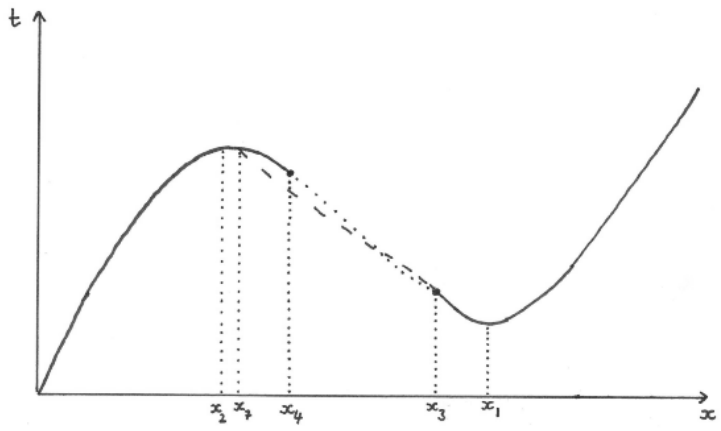

FIGURE 4. Solid curve: $s_0(t)$ as determined by the Hamilton-Jacobi mechanism. Dashed curve: $s_0(t)$ as determined by the repeated-root mechanism. The solid curve in $x_7 < x < x_4$ plays no role, being superceded by the self-sustaining repeated-root front. Dotted curve: $x = \omega(t)$ in $x_3 < x < x_4$; note from (107) that $\dot{\omega} < -2\Psi^{\frac{1}{2}}(\omega)$ holds close to x_3.

5. **Loose ends.** We wish to touch on a number of further issues here without exploring all their ramifications. We shall omit any discussion of traditional pushed fronts (whereby the wavespeed that is realised in greater than that accessible by linear methods), referring to [2] for a discussion of some of the issues, and of the higher-dimensional case even though many of the results carry over rather directly.

Firstly, we revisit the pulled front/pushed front concepts frequently adopted in the case of homogenous PDEs (see references in [2], including [3]). The current analysis suggests a somewhat different such classification, based very explicitly on the nature of the dominant rays: wavefronts selected by the Hamilton-Jacobi mechanisms are associated with rays that enter the front having passed through a region in which u is exponentially small – this information flow into the front is in keeping with the intuition behind a pulled front, namely the rate at which it is dragged forward is determined by the linearised response ahead of it. Conversely, in the repeated-root mechanism the rays that dominate the solution immediately ahead of the front emerge from the front itself (carrying information out from, rather than in to, the front) and have no analog for the linearised PDE, reflecting the nonlinear phenomenon of a self-sustaining propagating wave (albeit one whose speed can be determined by linearisation of the travelling-wave ODE) – such behaviour is more in keeping with the concepts conventionally associated with a pushed front. This distinction is thus very clean-cut and can be concisely expressed (Hamilton-Jacobi selection: dominant rays enter the front; repeated-root selection: dominant rays depart the front); the homogenous case is exceptional in that the rays neither enter nor leave the wavefront (i.e. the wavefront is itself a ray), complicating any such classification.

A number of ray families is present: we have described in detail the roles of the expansion-fan family and of the rays emerging from and outrunning a repeated-root front. Others are as follows. (i) For initial data of the form

$$\ln u \sim -f_0(x)/\varepsilon \quad \text{as} \quad \varepsilon \to 0 \tag{110}$$

for sufficient large x, the solution to (56) subject to $f = f_0(x) > 0$ at $t = 0$ is needed and may for the usual reasons (for sufficiently slowly decaying initial data) drive the front faster than the preceding calculations imply (one simply determines whether the $f = 0$ level set associated with (110) outruns the wavefront associated with the results of Section 3); (ii) rays propagating out of the wavefront – as we have seen, for repeated root fronts these emerge tangentially, whereas for the Hamilton-Jacobi mechanism they are associated with the positive square root in (52) i.e. with the fast-decaying exponential in the tail of the travelling wave, having from (57) that on rays

$$\frac{dx}{dt} = \dot{s} + (\dot{s}^2 - 4\Psi(s))^{\frac{1}{2}} \quad \text{as} \quad x = s(t),$$

i.e. the rays emerge moving faster than the wavefront (in contrast to the negative square root discussed above for which the rays enter the wavefront; revisiting the viewpoint whereby the nonlinearity acts as an obstacle, the former are analogous to reflections of the latter); these rays initially have u exponentially small but could in principle determine the location of a wavefront if f subsequently drops below zero, a possibility that we have not explored in any detail; (iii) reflected rays associated with exponentially small contributions (due to the Stokes phenomenon and associated in the usual way with reflection from waves propagating into a spatially slowly varying medium) will be present, but seem unlikely to play any role in wavefront selection; (iv) complex rays (again associated with exponentially small contributions) can occur, notably those lying beyond the caustic when a ray envelop is present. A comprehensive procedure would seem likely to require computing the solutions to (56) associated with each of the possible ray families, rejecting at each time t any that satisfy (70) and determining which of the remainder has $f = 0$ at the largest value of x, which is then identified with $s_0(t)$; in view of (ii), additional families then need to be considered if the mechanism by which $x = s_0(t)$ is selected switches.

While we have chosen to focus here on monotonic $\Psi(x)$, it is relevant to make a number of comments about more general Ψ, not least because leftward moving additional fronts that can arise when $\Psi' > 0$ (see Section 4) have features in common with the non-monotonic case. Periodic $\Psi(x)$ is the most widely studied example and in this regard we limit ourselves to commenting that the interplay between the two limits (i.e. $\varepsilon \to 0$ and $t \to +\infty$) then leads to issues that we shall not pursue here, associated in particular with the additional rays that emanate from the front. Our remaining comments concern what happens when Ψ' changes sign. Firstly, if Ψ' starts negative and then switches to positive (at $x_c = s_0(t_c)$, say) then the repeated-root condition that holds for $t < t_c$ necessarily ceases to be valid as soon as t passes through t_c (contrast the second case below). The transition is described by the following canonical inner problem: the appropriate scalings are

$$x = s(T, \varepsilon) + \varepsilon^{\frac{3}{5}} Z, \quad t = t_c + \varepsilon^{\frac{1}{5}} T, \quad u = \frac{1}{\varepsilon^{\frac{2}{5}}} e^{-\frac{Z}{2\varepsilon^{3/5}} \frac{ds}{dT}},$$

and, taking

$$\Psi \sim \Psi_c + \mu_c (x - x_c)^2 + \nu_c (x - x_c)^3 + \kappa_c (x - x_c)^4 \quad \text{as} \quad x \to x_c,$$

with $\mu_c > 0$ (it is noteworthy how many terms must be accounted for in this expansion), we find that

$$s(T, \varepsilon) \sim x_c + 2\varepsilon^{\frac{1}{5}} \Psi_c^{\frac{1}{2}} T + \frac{4}{3} \varepsilon^{\frac{3}{5}} \mu_c \Psi_c^{\frac{1}{2}} T^3 + 2\varepsilon^{\frac{4}{5}} \nu_c \Psi_c T^4 + \varepsilon S(T),$$

wherein the first four terms on the right-hand side coincide with those arising from the repeated-root condition (53). These scalings yield the leading-order problem

$$\frac{\partial v_0}{\partial T} = \frac{\partial^2 v_0}{\partial Z^2} + \left(8\mu_c \Psi_c^{\frac{1}{2}} ZT + \left(\frac{4}{3}\mu_c^2 \Psi_c + 16\kappa_c \Psi_c^2\right) - \Psi_c^{\frac{1}{2}} \frac{dS}{dT}\right) v_0. \tag{111}$$

The $T \to -\infty$ behaviour of (111), which represents the first of the two canonical PDEs that we record in the section, is given by (86); the most significant feature of (111) is the switch in sign of the Zv_0 term as T passes through zero. The associated ray picture as $T \to +\infty$ involves rays that depart tangentially from the repeated-root front when $t < t_c$ reentering the front with $t > t_c$, with these (rather than expansion-fan rays) mediating the Hamilton-Jacobi selection mechanism there; these rays cannot cross each other while $p > 0$: given (71) we have

$$\dot{x} = 2\left(2\Psi(s_0(t_0)) - \Psi(x)\right)^{\frac{1}{2}}$$

for the ray departing the front at $t = t_0 < t_c$, the ray velocity for given x decreasing as t_0 increases.

Secondly, if Ψ' starts positive and then becomes negative at $x = x_c$ the Hamilton-Jacobi selection mechanism remains valid for $x - x_c$ positive but sufficiently small; if a switch to the repeated-root mechanism occurs it does so at the point $x = x_s > x_c$ at which the relevant expansion-fan ray touches $s_0(t)$ tangentially (it is only at such an exceptional point that equality in (65) can arise for the Hamilton-Jacobi mechanism). Taking

$$\Psi \sim \Psi_s - \mu_s(x - x_s) + \nu_s(x - x_s)^2 \quad \text{as} \quad x \to x_s$$

with $\mu_s > 0$, we find from (56) that

$$f \sim \Psi_s^{\frac{1}{2}}(x - x_s) - 2\Psi_s(t - t_s) + \mu_s(x - x_s - \Psi_s^{\frac{1}{2}}(t - t_s))(t - t_s) + \frac{1}{2}\frac{\partial p}{\partial x}(x_s, t_s)(x - x_s - 2\Psi_s^{\frac{1}{2}}(t - t_s))^2$$

as $t \to t_s^-$ with $x_s - x = O(t_s - t)$ where $x_s = s_0(t_s)$, so that

$$s_0(t) \sim x_s - 2\Psi_s^{\frac{1}{2}}(t_s - t) - \mu_s(t_s - t)^2 \quad \text{as} \quad t \to t_s^-.$$

The inner scalings that apply in this case are

$$x = s(T;\varepsilon) + \varepsilon^{2/3} Z,\ t = t_s + \varepsilon^{1/3} T,\ u = \frac{1}{\varepsilon^{1/3}} e^{-\frac{Z}{2\varepsilon^{2/3}}\frac{ds}{dT}} v,$$

and we find that

$$s \sim x_s + 2\varepsilon^{\frac{1}{3}}\Psi_s^{\frac{1}{2}} T - \varepsilon^{\frac{2}{3}}\mu_s T^2 + \varepsilon S(T),$$

and obtain the second of the canonical PDEs here in the form

$$\frac{\partial v_0}{\partial T} = \frac{\partial^2 v_0}{\partial Z^2} + \left(-2\mu_s ZT + 4\nu_s \Psi_s T^2 - \Psi_s^{\frac{1}{2}}\frac{dS}{dT}\right) v_0, \tag{112}$$

now consistent with (86) as $T \to +\infty$, in which limit the rays emerge tangentially from the front.

A much more general remark to which we return below is the following. Many of the concepts described here go over to cases involving higher-order systems, but the situation can be much more complicated not just because there are typically more ray families but, even more importantly, because the dominant rays may be complex ones, the wavefront being associated with the level set $\mathrm{Re}(f) = 0$, rather than simply $f = 0$, and hence with modulated travelling waves instead of waves of

fixed form (even more complicated possibilities can arise, of course). The Stokes phenomenon potentially plays a significant role here also.

As a minor remark, we note that the Hamilton-Jacobi equation

$$\frac{\partial f}{\partial t} + \left(\frac{\partial f}{\partial x}\right)^2 + (1-\theta)\Psi(x) + \theta = 0$$

associated with the linearised equation

$$\varepsilon \frac{\partial U}{\partial t} = \varepsilon^2 \frac{\partial^2 U}{\partial x^2} + ((1-\theta)\Psi(x) + \theta)U$$

is mapped for constant θ to (56) by the equivalence transformation

$$f \to -\theta t + (1-\theta)^{\frac{1}{2}} f, \quad t \to (1-\theta)^{-\frac{1}{2}} \hat{t}$$

providing a simple relationship within a class of heterogeneities.

The front profile when the repeated-root mechanism applies is that of the minimum speed non-negative travelling wave; faster waves can be realised for slowly decaying data whichever wavespeed selection mechanism applies. For the Hamilton-Jacobi mechanism, however, the front propagates faster than the minimum wavespeed no matter how rapidly the initial data decay and it is natural to consider why more slowly moving fronts cannot be realised: this can be investigated simply by solving (56) for decreasing t from a wavefront whose speed lies between the Hamilton-Jacobi and repeated-root values (it is noteworthy that, in contrast to (2), there is little difficulty in running the eikonal equation (56) backward in time): the rays associated with (64) bend around to collide with the front at some smaller positive t, and have an envelope below which they cease to be real; as the wavespeed drops to the repeated-root value this envelope approaches the wavefront itself. Since there is no information flow ahead of the envelope via these rays, were the expansion fan (which, were it present, would enforce a faster-propagating wave) to be absent then a zone of silence would result – in other words, while such wavefronts appear to represent asymptotically self-consistent solutions locally, it does not seem possible to match them forward into a meaningful tail region in which u is exponentially small: they are thus slightly curious objects from the point of view of intermediate-asymptotic PDE theory.

6. **Discussion.** It is important to emphasise that the key result of the above analysis is not simply that the front velocity depends on Ψ (which is obvious) but that the mechanism by which it is selected depends crucially on the sign of Ψ'. Formal derivations of the wavespeed for Fisher's equation differ between communities: mathematical-biology texts tend to appeal to a phase-plane analysis of the travelling-wave ODE, whereas the physics literature often adopts a steepest-descent approach to a Fourier-transform-based integral representation[11] of the solution to a (spatially homogeneous) linearised system, reflecting respectively the repeated-root and Hamilton-Jacobi mechanisms; that these exceptionally give the same result for the homogeneous PDE has led to the clear differences between these two mechanisms often being overlooked.

We have sought to demonstrate in the above how geometrical optics, and canonical inner problems of the type that arise in the geometrical theory of diffraction

[11] Such a non-local representation is already somewhat moot, given that the linearisation is self-evidently inapplicable behind the wavefront; the local information flow explicit from the Hamilton-Jacobi approach clarifies the circumstances under which the results are applicable.

(GTD), can be crucial to the formal understanding of wave propagation in parabolic systems, the associated ray-based insight into information flow providing a viewpoint that is relatively rarely exploited. Many phenomena familiar from linear diffraction theory play a central role (refraction, total internal reflection, caustics etc.) and the Liouville-Green approach adopted here explicitly invokes the linearised PDE. Nevertheless, it is important also to highlight two intrinsically nonlinear effects that are crucial in understanding the full ray picture for the linearised PDE. Firstly, a new ray field is shed by a (self-sustaining and self-limiting) repeated-root front (and indeed also by conventional pushed fronts): this has no analog for the linearised PDE, the large-time behaviour of which sheds no light on the nonlinear wavespeed (put more bluntly: for $\Psi' < 0$ the large-time analysis of the linearised PDE gives the wrong answer, as does a naïve phase-plane analysis of the travelling-wave ODE when $\Psi' > 0$ in the sense that the minimum permitted wavespeed identified by the phase-plane analysis is not in fact realised). Secondly, the condition (70) for the inadmissibility of rays does not arise in the linear case and can be interpreted as expressing their annihilation on confronting the nonlinearity[12] (while related rays may reemerge in a modified form on the other side of the wavefront, they are not relevant to the current discussion); by contrast, on the anti-Stokes lines of linear problems (these being curves on which two exponential contributions are equal in size) each set of rays passes through unaltered (in contrast to the Stokes lines across which the rays associated with a (maximally) subdominant contribution can be entirely deactivated). Such effects have implications way beyond the very specific class of problems addressed here.

Even for this specific class, there are a number of questions that we have not attempted to resolve here even at a formal level, of which we highlight three. Firstly, from (73) we have that the wavefront necessarily decelerates when $\Psi' < 0$; for $\Psi' > 0$, it is clear from the fact that newly initiated fronts start off with unbounded velocity that the wavefront need not necessarily accelerate (that this is also true even when no new fronts form follows from consideration of cases in which they just fail to do so), but it would be worthwhile to determine what can be said about $\ddot{s}_0$ or related quantities (perhaps in terms of the sign of Ψ'', for example). Secondly, the analysis in Section 5 implies that when Ψ' switches from negative to positive, the rays shed by the repeated-root front are responsible for wavespeed selection in the subsequent Hamilton-Jacobi front: an open question alluded to in Section 5 concerns cataloguing the circumstances under which rays emerging from a front (including those associated with fast-decay from a Hamilton-Jacobi front) can govern subsequent front behaviour. Finally, a more detailed classification of when additional fronts will arise might be instructive.

In keeping with our goal of establishing a GTD-related framework for addressing problems of the current type, we have paid particular attention to formulating canonical inner problems that play roles that are in some sense universal (though we stress that we have not sought a comprehensive classification of these); it is striking that in most cases (such as (86), (111) and (112)) these are linear.

In concluding, we emphasis the very broad applicability of the new distinct mechanisms identified here in characterising nonlinear waves propagating over unstable

[12]In other words and as already noted, the nonlinearity acts as a self-generating (rather than externally prescribed) obstacle preventing the further propagation of the rays of the linearised problem.

states and susceptible to classification by linear methods[13]. The generalisation of the repeated-root mechanism to higher-order systems typically involving extending the permanent-form travelling-wave ansatz to that for modulated travelling waves (MTWs) i.e. considering local solutions of the form

$$\phi(z,t;c,T) \text{ with } \phi(z,t+T;c,T)=\phi(z,t;c,T) \tag{113}$$

in some suitable local travelling-wave coordinate z, linearising the MTW PDE and determining the two real quantities c and T and the (in general complex) decay rate of ϕ from the two complex equations made up of the auxiliary equation for the decay rate (obtained by separation of variables with the time-dependence constrained by (113)) and the associated repeated-root condition. For the Hamilton-Jacobi mechanism, one obtains the expansion-fan solutions to the relevant eikonal equation and determines the level sets $\mathrm{Re}(f)=0$ as putative markers for the wavefront location (with the value of $\mathrm{Im}(f)$ there implying the local periodicity in t in the case of a MTW; the inadmissibility condition (70) for the Hamilton-Jacobi mechanism generalises to involve $\mathrm{Re}(f(x,t^{'}))<0$): that the eikonal equation will typically have multiple branches, and that careful account must be taken of complex rays and of the Stokes phenomenon, illustrates the far from trivial additional steps that must be undertaken in such cases (a related proviso applies for the repeated-root case also since the relevant condition can be satisfied by a discrete set of wavespeeds and, moreover, non-negativity of the wave profile cannot be used as a criterion when there is no suitable comparison principle). In the spatially homogeneous cases that have been most widely studied, these two mechanisms give the same wavespeed, but this is not the case more generally: a large part of our motivation for considering the relatively simple specific case (2) in detail was to highlight the distinctiveness and complementarity of the two mechanisms, thereby providing insight into their comprehensiveness and generic applicability.

7. **Acknowledgments.** I am grateful to Carlota Cuesta for helpful discussions and to the Royal Society and Wolfson Foundation for funding.

Appendix 1 A distinguished limit. For obvious reasons, we have taken Ψ above to be independent of ε. Here we instead briefly discuss the case

$$\Psi(x;\varepsilon)=1+\varepsilon^{\frac{1}{2}}\psi(x), \quad \psi(0)=0, \tag{A1.1}$$

which is distinguished in the sense that it describes the transition between the two cases discussed in detail above in the limit $\varepsilon\to 0$ with $t=O(1)$. The analysis closely parallels that of Section 2.2.

We set (for $t=O(1)$)

$$x=s(t;\varepsilon)+\varepsilon^{\frac{1}{2}}\zeta, \quad s(t;\varepsilon)\sim 2t+\varepsilon^{\frac{1}{2}}s_1(t)+\varepsilon\ln(1/\varepsilon)s_2(t)+\varepsilon s_3(t), \tag{A1.2}$$

and

$$u=\frac{e^{-\zeta/\varepsilon^{\frac{1}{2}}}}{\varepsilon^{1/2}}v$$

in the linearised PDE to give (retaining terms up to $O(\varepsilon^{\frac{1}{2}})$)

$$\varepsilon^{\frac{1}{2}}\frac{\partial v}{\partial t}+(\dot{s}_1+\varepsilon^{\frac{1}{2}}\ln(1/\varepsilon)\dot{s}_2+\varepsilon^{\frac{1}{2}}\dot{s}_3)v-\varepsilon^{\frac{1}{2}}\dot{s}_1\frac{\partial v}{\partial\zeta}\sim\varepsilon^{\frac{1}{2}}\frac{\partial^2 v}{\partial\zeta^2}+\psi(2t)v+\varepsilon^{\frac{1}{2}}(s_1+\zeta)\psi^{'}(2t)v.$$

[13]By this we exclude situations in which a pushed (nonlinearity selected) front arises, i.e. when, in the case of higher-order systems, the corresponding analogue of the scenario summarised in footnote 3 pertains.

hence

$$s_1(t) = \int_0^t \psi(2t')dt', \quad s_2(t) = -\frac{3}{2}, \tag{A1.3}$$

and

$$\begin{aligned} &\frac{\partial v_0}{\partial t} = \frac{\partial^2 v_0}{\partial \zeta^2} + \psi(2t)\frac{\partial v_0}{\partial \zeta} + (s_1(t)\psi'(2t) - \dot{s}_3(t) + \psi'(2t)\zeta)v_0, \\ &\text{as } \zeta \to 0^+ \quad v_0 \sim K\zeta, \\ &\text{as } t \to 0^+ \quad v_0 \sim K\zeta e^{-\zeta^2/4t}, \end{aligned} \tag{A1.4}$$

which (cf. (33)) determines $s_3(t)$ as well as $v_0(\zeta, t)$. The formulation (A1.4) can be simplified somewhat by setting

$$v_0 = \exp\left(-\frac{1}{2}\psi(2t)\zeta + \int_0^t \left(s_1(t')\psi'(2t') - \frac{1}{4}\psi^2(2t')\right)dt' - s_3(t)\right) w$$

to give

$$\begin{aligned} &\frac{\partial w}{\partial t} = \frac{\partial^2 w}{\partial \zeta^2} + 2\psi'(2t)\zeta w, \\ &\text{at } \zeta = 0 \quad w = 0, \\ &\text{as } t \to 0^+ \; w \sim \frac{I_1}{t^{\frac{3}{2}}}\zeta e^{-\zeta^2/4t}, \end{aligned} \tag{A1.5}$$

where I_1 corresponds to that in Section 2.1.

Analysing (A1.5) for large ψ reestablishes the subdivision between the cases $\Psi' > 0$ and $\Psi' < 0$, but for $\psi = O(1)$ no further simplification is possible for $t = O(1)$. The key point to emphasise is then as follows: in (A1.1) the heterogeneity is both small and slowly varying, so the behaviour could be expected very closely to follow that of the classical homogeneous case; nevertheless, the correction term $s_3(t)$ is sensitive to the form of $\psi(x)$, as expressed by (A1.4) – in this sense, considerable caution needs to be exercised in the application of universality results such as those of [3] beyond the context in which they were derived. A further cautionary example is provided by the case $\varepsilon = 1, \Psi(x) \sim 1 + \mu/x$ as $x \to +\infty$ for which the logarithmic term in the large-time expansion for $s(t)$ depends on the value of the constant μ.

Appendix 2 Piecewise-constant heterogeneity. Here we consider the instructive special case

$$\Psi(x) \equiv 1 \quad \text{for} \quad 0 < x < 1, \quad \Psi(x) \equiv \Psi_\infty \quad \text{for} \quad x > 1, \tag{A2.1}$$

aspects of which have been investigated by [6]. While $x < 1$, the expansion fan solution is given by

$$x = 2p_0 t, \quad f = (p_0^2 - 1)t = \frac{x^2}{4t} - t, \quad A = \frac{1}{t^{1/2}} a\left(\frac{x}{t}\right), \quad t < 1/2p_0. \tag{A2.2}$$

Since $q = \partial f/\partial t$ is constant on rays, those that pass through $x = 1$ are refracted and have

$$p = (p_0^2 + 1 - \Psi_\infty)^{\frac{1}{2}} \quad \text{for} \quad t > 1/2p_0,$$

i.e. they require that $p_0^2 > \Psi_\infty - 1$, and on such rays f is given parametrically in terms of p_0 by

$$x = 2(p_0^2 + 1 - \Psi_\infty)^{\frac{1}{2}}\left(t - \frac{1}{2p_0}\right) + 1, \; f = (p_0^2 + 1 - 2\Psi_\infty)t + \frac{1}{p_0}(\Psi_\infty - 1) \tag{A2.3}$$

for $t > 1/2p_0$. The most significant ray for what follows is that corresponding to $p_0 = p^* \equiv (\Psi_\infty - 1)^{\frac{1}{2}}$ for which (A2.3) reduces to

$$x = 1, \quad f = -\Psi_\infty t + (\Psi_\infty + 1)^{\frac{1}{2}} \quad \text{for} \quad t > 1/2(\Psi_\infty - 1)^{\frac{1}{2}}. \tag{A2.4}$$

This identifies $\Psi_\infty = 2$ as a borderline value: for $1 < \Psi_\infty < 2$ we have $p^* < 1$ and (A2.4) has $f < 0$ for all $t > t^\dagger \equiv 1/2p^*$, whereas for $\Psi_\infty > 2$, $p^* > 1$ and (A2.4) passes through zero from above at $t = t^* \equiv (\Psi_\infty - 1)^{\frac{1}{2}}/\Psi_\infty$, where $t^* < 1/2$: as we shall see, this corresponds to the nucleation of additional fronts.

The front location in $x < 1$ follows at once from (A2.2), corresponding to $p_0 = 1$ and hence

$$s_0(t) = 2t \quad \text{for} \quad t < 1/2. \tag{A2.5}$$

For $1 < \Psi_\infty < 2$ propagation proceeds continuously into $x > 1$, with $s_0(t)$ given parametrically by

$$s_0(t) = 2(p_0^2 + 1 - \Psi_\infty)^{\frac{1}{2}} \left(t - \frac{1}{2p_0}\right) + 1, \; 0 = (p_0^2 + 1 - 2\Psi_\infty)t + \frac{1}{p_0}(\Psi_\infty - 1) \text{ for } t > 1/2; \tag{A2.6}$$

from (A2.6) we have that p_0 is a monotonically increasing function of t with

$$p_0 \sim 1 + \frac{2(\Psi_\infty - 1)}{(2 - \Psi_\infty)}\left(t - \frac{1}{2}\right), \quad s_0(t) \sim 1 + \frac{2}{(2 - \Psi_\infty)^{\frac{1}{2}}}\left(t - \frac{1}{2}\right) \quad \text{as} \quad t \to \frac{1}{2}^+, \tag{A2.7}$$

from which the requirement that $\Psi_\infty < 2$ holds is immediate and

$$p_0 \sim (2\Psi_\infty - 1)^{\frac{1}{2}}, \quad s_0(t) \sim 2\Psi_\infty^{\frac{1}{2}} t \quad \text{as} \quad t \to +\infty, \tag{A2.8}$$

as is to be expected. The velocity thus jumps discontinuously to its maximum value as s_0 passes through 1 and then decreases.

For $\Psi_\infty > 2$ new wavefronts are born at $x = 1$, $t = t^*$. The one that propagates to the right is determined by the Hamilton-Jacobi selection mechanism, so is given by (A2.6) and satisfies

$$\begin{aligned} p_0 &\sim (\Psi_\infty - 1)^{\frac{1}{2}} + \frac{\Psi_\infty^2}{(\Psi_\infty - 2)}(t - t^*), \\ s_0(t) &\sim 1 + \left(\frac{2(\Psi_\infty - 2)}{(\Psi_\infty - 1)^{\frac{1}{2}}}\right)^{\frac{1}{2}} (t - t^*)^{\frac{1}{2}} \quad \text{as} \quad t \to {t^*}^+, \end{aligned} \tag{A2.9}$$

the requirement that $\Psi_\infty > 2$ being immediately apparent, and (A2.8). Alongside (A2.9) we have

$$f(x,t) \sim \frac{\Psi_\infty(\Psi_\infty - 2)^{\frac{1}{2}}}{2(\Psi_\infty - 2)}(x-1)^2 - \Psi_\infty(t - t^*) \quad \text{as} \quad x \to 1^+, t \to {t^*}^+. \tag{A2.10}$$

Thus the speed is unbounded at $t = t^*$ and subsequently decreases to $2\Psi_\infty^{\frac{1}{2}}$. The leftward moving front has no analog for the linear PDE theory and is in effect determined by the repeated-root mechanism, being given by

$$s_0(t) = 1 - 2(t - t^*) \quad \text{for} \quad t^* < t < (1 + 2t^*)/4,$$

colliding with the original front (A2.5) at $t = (1 + 2t^*)/4$, after which time the only front is the one in $x > 1$, given by (A2.6).

Finally, in the borderline case $\Psi_\infty = 2$ we find that

$$p_0 \sim 1+2\left(\frac{1}{3}\left(t-\frac{1}{2}\right)\right)^{\frac{1}{2}}, \quad s_0(t) \sim 1+4\left(\frac{1}{3}\left(t-\frac{1}{2}\right)\right)^{\frac{3}{4}} \quad \text{as} \quad t \to \frac{1}{2}^+ \tag{A2.11}$$

together with (A2.8). Thus, as for (A2.9) the interface velocity is unbounded as s_0 passes through 1, but (A2.11), unlike (A2.9), exhibits continuity with (A2.5). In addition

$$f(x,t) \sim \frac{3}{2^{5/3}}(x-1)^{\frac{4}{3}} - 2\left(t-\frac{1}{2}\right) \quad \text{as} \quad x \to 1^+, t \to \frac{1}{2}^+.$$

Rays with $p_0^2 < \Psi_\infty - 1$ suffer total internal reflection at $x = 1, p$ becoming $-p_0$ (hence maintaining the value of $q = -p^2 - 1$) on hitting $x = 1$, so that the ray propagates back into $x < 1$. The critical ray (on which $p_0 = p^*$) also sheds rays having $p = -p^*$ back into $x < 1$ for each value of $t > t^\dagger$; however, none of these backward propagating rays plays a role in wavefront selection and we do not discuss them further.

The final issue we shall discuss here is associated with the initiation of the two additional fronts at $x = 1$, $t = t^*$, since the inner problem that describes this plays a role akin to that of a canonical diffraction problem in geometric optics, but has no analog in the linear PDE. To accomplish this, we first need to characterise the behaviour of the solution close to $x = 1$. For $t < t^\dagger < t^*$ we have from (A2.2) that

$$u \sim \frac{\varepsilon^{1/2}}{t^{1/2}} a\left(\frac{1}{t}\right)\, e^{(t-1/4t)/\varepsilon}\, e^{-X/2t} \quad \text{for} \quad X = O(1)$$

where $x = 1 + \varepsilon X$. Setting

$$u = \frac{\varepsilon^{1/2}}{t^{1/2}} a\left(\frac{1}{t}\right)\, e^{(t-1/4t)/\varepsilon}\, v(X,t)$$

gives

$$\frac{\partial^2 v_0}{\partial X^2} = \frac{1}{4t^2} v_0, \ X < 0, \ \frac{\partial^2 v_0}{\partial X^2} = \left(1 + \frac{1}{4t^2} - \Psi_\infty\right) v_0, \ X > 0$$

so that

$$v_0 = e^{-X/2t} + \frac{1-(1-4(\Psi_\infty-1)t^2)^{\frac{1}{2}}}{1+(1-4(\Psi_\infty-1)t^2)^{\frac{1}{2}}}\, e^{X/2t}, \ X < 0 \tag{A2.12}$$

the second term in which represents a reflected field that is not significant here since it decays exponentially as X decreases; a reflected field will also be present for smooth $\Psi(x)$, but can for the usual reasons be expected to be multiplied by a prefactor that is exponentially small in ε – such behaviour is of interest in its own right but is not germaine here. The transmitted field corresponding to (A2.12) is

$$v_0 = \frac{2}{1+(1-4(\Psi_\infty-1)t^2)^{\frac{1}{2}}}\, \exp\left(-\frac{1}{2t}(1-4(\Psi_\infty-1)t^2)^{\frac{1}{2}} X\right), \ X > 0; \tag{A2.13}$$

this ceases to be exponentially decaying at $t = t^\dagger$, leading to a canonical 'diffraction' problem for t close to $t^\dagger$ that is again of interest in its own right but is relegated to Appendix 3 because it is a problem exclusively in linear PDE theory.

For $t^\dagger < t < t^*$ the behaviour for $|x-1| \ll 1$ is dictated by rays close to the critical one corresponding to $p = p^*$: setting $p_0 = p^*(1+\delta)$ where δ is an artificial

small parameter yields from (A2.3) that

$$x \sim 1 + 2^{3/2} p^* \delta^{\frac{1}{2}} (t - t^\dagger), \; f \sim \frac{(x-1)^2}{4(t-t^\dagger)} - \Psi_\infty (t - t^*) \quad \text{as} \quad x \to 1^+, \tag{A2.14}$$

having (A2.10) as a special case. There are now two additional regions close to $x = 1$. Firstly, we set $x = 1 + \varepsilon^{1/2} Y$ with $Y > 0$ and

$$u = \Lambda(\varepsilon) e^{\Psi_\infty (t-t^*)/\varepsilon} W(Y, t), \tag{A2.15}$$

where calculating the quantity $\Lambda(\varepsilon)$ requires analysis of the inner problem at $t = t^\dagger$ (see Appendix 3). At leading order we have for $t^\dagger < t < t^*$

$$\begin{aligned} \frac{\partial W_0}{\partial t} &= \frac{\partial^2 W_0}{\partial Y^2}, \\ \text{at} \quad Y = 0 \; W_0 &= 0, \end{aligned}$$

where the condition at $Y = 0$ follows from matching into the $X = O(1)$ region described next, and hence

$$W_0 = \frac{Y}{(t-t^\dagger)^{3/2}} \; e^{-Y^2/4(t-t^\dagger)}, \tag{A2.16}$$

given the results of Appendix 3, which yield on matching into (A2.16) that

$$\Lambda(\varepsilon) \sim \varepsilon \frac{a(2p^*)}{2p^*}.$$

The second region has $X = O(1)$ with

$$u = \varepsilon^{\frac{1}{2}} \Lambda(\varepsilon) \; e^{\Psi_\infty (t-t^*)/\varepsilon} \; V(X, t)$$

and at leading order

$$\frac{\partial^2 V_0}{\partial X^2} = (\Psi_\infty - 1) V_0, \quad X < 0, \quad \frac{\partial^2 V_0}{\partial X^2} = 0, \quad X > 0$$

so that

$$V_0 = \frac{1}{p^* (t-t^\dagger)^{3/2}} e^{p^* X}, \quad X < 0, \quad V_0 = \frac{1}{p^* (t-t^\dagger)^{3/2}} \; (1 + p^* X), \quad X > 0 \tag{A2.17}$$

on matching with (A2.16). The first of (A2.17) generates a reflected field in $x < 1$[14]; this and the totally internally reflected field arising for $p_0 < p^*$ should be contrasted with that present in (A2.12) in that rays analogous to the former are also relevant in the case of smooth $\Psi(x)$: considering the case in which Ψ increases rapidly but smoothly from 1 to Ψ_∞ in the neighbourhood of $x = 1$, rays with p just less than p^* hug $x = 1$ while those with smaller p turn around more rapidly – the role of rays which swap direction has been discussed above.

Evidently, (A2.15) ceases to be small when t approaches t^* and u becomes of $O(1)$. Setting

$$t = t^* - \frac{\varepsilon}{\Psi_\infty} \ln \Lambda + \varepsilon T$$

we have in $Y = O(1)$ with $Y > 0$

$$\frac{\partial u_0}{\partial T} = \Psi_\infty u_0 (1 - u_0)$$

[14]It is reflected at the critical angle, with the ray with $p_0 = p^*$ being that analogous to that associated with the head wave in descriptions of seismic wave propagation, for example.

$$\text{as} \quad T \to -\infty \quad u_0 \sim \frac{Y}{(t^* - t^\dagger)^{\frac{3}{2}}}\, e^{-Y^2/4(t^*-t^\dagger)}$$

so the rightward moving front satisfies

$$Y \sim 2(\Psi_\infty(t^* - t^\dagger)T)^{\frac{1}{2}} \quad \text{as} \quad T \to +\infty;$$

since

$$t^* - t^\dagger = \frac{\Psi_\infty - 2}{2\Psi_\infty(\Psi_\infty - 1)^{\frac{1}{2}}},$$

this is consistent with (A2.9). As $Y \to 0^+$ we have

$$u_0 \sim \frac{Y}{(t^* - t^\dagger)^{\frac{3}{2}}} e^{\Psi_\infty T} \tag{A2.18}$$

for $T = O(1)$, and to initiate the leftward moving front we need to take account of (A2.17) by setting

$$T = \frac{1}{2\Psi_\infty}\ln(1/\varepsilon) + \frac{3}{2\Psi_\infty}\ln(t^* - t^\dagger) + \hat{T}$$

to give the canonical *nonlinear* 'diffraction' problem

$$\frac{\partial u_0}{\partial \hat{T}} = \frac{\partial^2 u_0}{\partial X^2} + (1 + H(X)(\Psi_\infty - 1))\, u_0(1 - u_0),$$

$$\text{as} \quad X \to -\infty \quad u_0 \to 0, \qquad \text{as} \quad X \to +\infty \quad u_0 \to 1,$$

where $H(X)$ is the Heaviside step function, subject to the initial data

$$u_0 \sim \frac{1}{p^*} e^{\Psi_\infty \hat{T} + p^* X} \quad \text{as} \quad \hat{T} \to -\infty, \quad X = O(1) \quad \text{with} \quad X < 0,$$

$$u_0 \sim \frac{1}{p^*} e^{\Psi_\infty \hat{T}}(1 + p^* X) \quad \text{as} \quad \hat{T} \to -\infty, \quad X = O(1) \quad \text{with} \quad X > 0,$$

$$u_0 \sim e^{\Psi_\infty \hat{T}} X/(1 + e^{\Psi_\infty \hat{T}} X) \quad \text{as} \quad \hat{T} \to -\infty, \quad X = O(e^{-\Psi_\infty \hat{T}}) \quad \text{with} \quad X > 0,$$

where we have made use of (A2.18). Since $p^* > 1$, the rate of exponential decay in the initial data as $X \to -\infty$ ensures that the leftward propagating wave is one of minimum speed, the location of which is therefore given by

$$X \sim -2\hat{T} + \frac{3}{2}\ln \hat{T} \quad \text{as} \quad \hat{T} \to +\infty.$$

This propagating wave has no analog in the linearised PDE, no indication of its location being provided by the original expansion-fan solution.

Appendix 3 A linear canonical inner problem. Here, as promised in Appendix 2, we analyse the behaviour close to $t = t^\dagger \equiv 1/2p^*$ for $\Psi_\infty > 2$, in part to emphasis how much analytical progres is possible with the techniques implemented here. First we set

$$p_0 = p^*(1 + \delta), \quad t = t^\dagger + \delta \hat{t} \tag{A3.1}$$

in (A2.3), where $\delta > 0$ is an artificial small parameter. Retaining terms in f up to $O(\delta^2)$ we find

$$x - 1 \sim 2^{\frac{1}{2}}\delta^{\frac{3}{2}}(2p^*\hat{t} + 1), \quad f \sim \Psi_\infty(t^* - t^\dagger) - \delta\Psi_\infty \hat{t} + \delta^2 p^* \left(2p^*\hat{t} + \frac{3}{2}\right). \tag{A3.2}$$

At $\hat{t} = 0$ we therefore have

$$f(x, t^\dagger) \sim \Psi_\infty(t^* - t^\dagger) + \frac{3p^*}{2^{5/3}}(x - 1)^{\frac{4}{3}} \quad \text{as} \quad x \to 1^+ \tag{A3.3}$$

while for $\hat{t} < 0$ (A3.2) takes the selfsimilar form

$$f(x,t) \sim \Psi_\infty(t^* - t^\dagger) + \Psi_\infty(t^\dagger - t) + (t^\dagger - t)^2 F_-(\eta_-) \quad \text{as} \quad t \to t^{\dagger^-},\ x \to 1^+ \tag{A3.4}$$

with the following parametric representation for $F_-(\eta_-)$

$$\eta_- = (x-1)/(t^\dagger - t)^{\frac{3}{2}}, \quad \eta_- = 2^{\frac{1}{2}}\mu_-^{\frac{3}{2}} - 2^{\frac{3}{2}}p^*\mu_-^{\frac{1}{2}}, F_-(\mu_-) = \frac{3}{2}p^*\mu_-^2 - 2p^{*^2}\mu_-, \tag{A3.5}$$

where $\delta = \mu_-(t^\dagger - t)$; similarly, for $\hat{t} > 0$ we have

$$f(x,t) \sim \Psi_\infty(t^* - t^\dagger) - \Psi_\infty(t - t^\dagger) + (t - t^\dagger)^2 F_+(\eta_+) \quad \text{as} \quad t \to t^{\dagger^+}, \quad x \to 1^+ \tag{A3.6}$$

with

$$\eta_+ = (x-1)/(t-t^\dagger)^{\frac{3}{2}}, \quad \eta_+ = 2^{\frac{1}{2}}\mu_+^{\frac{3}{2}} + 2^{\frac{3}{2}}p^*\mu_+^{\frac{1}{2}}, F_+(\eta_+) = \frac{3}{2}p^*\mu_+^2 + 2p^{*^2}\mu_+, \tag{A3.7}$$

where $\delta = \mu_+(t - t^*)$. Asymptotic expressions accordingly take the form

$$F_-(\eta) \sim \frac{3p^*}{2^{5/3}}\eta^{\frac{4}{3}} + 2^{2/3}p^{*^2}\eta^{\frac{2}{3}},\ F_+(\eta) \sim \frac{3p^*}{2^{5/3}}\eta^{\frac{4}{3}} - 2^{2/3}p^{*^2}\eta^{\frac{2}{3}} \quad \text{as} \quad \eta \to +\infty \tag{A3.8}$$

and

$$F_-(\eta) \sim 2p^{*3} + 2p^{*\frac{3}{2}}\eta, \quad F_+(\eta) \sim \frac{1}{4}\eta^2 \quad \text{as} \quad \eta \to 0^+, \tag{A3.9}$$

the first of (A3.9) correspond to $\mu_- \sim 2p^*$ and the second to $\mu_+ \sim \eta_+^2/8p^{*2}$.

From the scalings in (A3.4)-(A3.5), it is clear that the inner analysis requires us to set

$$x = 1 + \varepsilon^{\frac{3}{4}}X, \quad t = t^\dagger + \varepsilon^{\frac{1}{2}}T \tag{A3.10}$$

and, by (A3.2) or (A3.4),

$$u = \varepsilon^{1/2}(2p^*)^{\frac{1}{2}}a(2p^*)\ e^{-\Psi_\infty(t^* - t^\dagger)/\varepsilon}\ e^{\Psi_\infty T/\varepsilon^{\frac{1}{2}}}v \tag{A3.11}$$

to give

$$\frac{\partial v_0}{\partial T} = \frac{\partial^2 v_0}{\partial X^2} \quad \text{for} \quad X > 0. \tag{A3.12}$$

The $\varepsilon^{1/2}$ and other prefactors in (A3.11) are introduced for convenience in view of the incoming ray solution in $X < 0$, namely

$$u \sim \frac{\varepsilon^{\frac{1}{2}}}{t^{\frac{1}{2}}}a\left(\frac{x}{t}\right)e^{(t-x^2/4t)/\varepsilon}$$

which becomes

$$v \sim e^{-p^*X/\varepsilon^{\frac{1}{4}}}\ e^{-2p^*T^2} \tag{A3.13}$$

under the rescalings (A3.10)-(A3.11); it is no coincidence that time dependence in (A3.13) corresponds to the first term in F_- in (A3.9). For $T = O(1)$, $X < 0$ we need to introduce $\hat{X} = X/\varepsilon^{\frac{1}{4}}$ to give

$$\frac{\partial^2 v_0}{\partial \hat{X}^2} = p^{*^2}v_0 \quad \text{for} \quad \hat{X} < 0$$

so that

$$v_0 = (e^{-p^*\hat{X}} + e^{p^*\hat{X}})e^{-2p^*T^2} \tag{A3.14}$$

follows on applying the matching condition

$$\frac{\partial v_0}{\partial \hat{X}} = 0 \quad \text{on} \quad \hat{X} = 0. \tag{A3.15}$$

Thus (A3.12) is to be solved subject to

$$v_0 = 2e^{-2p^*T^2} \quad \text{on} \quad X = 0; \tag{A3.16}$$

in setting up the initial boundary value problem it is necessary also to determine the amplitude prefactor in $x > 1$, whereby u can for reasons noted above be expressed in the form

$$u \sim \varepsilon^{\frac{1}{2}} \left(-\frac{\partial^2 f}{\partial x \partial t}\right)^{\frac{1}{2}} \Omega\left(-\frac{\partial f}{\partial t}\right) e^{-f(x,t)/\varepsilon} \tag{A3.17}$$

for some function Ω. Since

$$q = -p_0^2 - 1, \quad p = (p_0^2 + 1 - \Psi_\infty)^{\frac{1}{2}}$$

and by (A3.1), (A3.3) we have

$$p_0 \sim p^* + 2p^{*^2}(t^\dagger - t) \quad \text{on} \quad x = 1 \quad \text{as} \quad t \to t^{\dagger^-},$$

it follows that

$$\frac{\partial f}{\partial t} \sim -\Psi_\infty - 4p^{*^3}(t^\dagger - t), \ \frac{\partial f}{\partial x} \sim 2p^{*^{\frac{3}{2}}}(t^\dagger - t)^{\frac{1}{2}}, \ \frac{\partial^2 f}{\partial x \partial t} \sim -p^{*^{\frac{3}{2}}}(t^\dagger - t)^{-\frac{1}{2}}$$

on $x = 1$ and consistency with (A3.16) as $T \to -\infty$ is readily seen to demand that

$$\Omega\left(-\frac{\partial f}{\partial t}\right) \sim \frac{2a(2p^*)}{p^*}\left(-\frac{\partial f}{\partial t} - \Psi_\infty\right)^{\frac{1}{4}}, \tag{A3.18}$$

this giving the amplitude carried by the rays that enter $x > 1$ when t is just less than $t^\dagger$. The significance of this result is that it provides the initial data on (A3.12), (A3.16) as $T \to -\infty$, namely

$$v_0 \sim \frac{1}{p^{*\frac{3}{2}}}\left(\frac{dF_-}{d\eta_-} - 3\eta_-\frac{d^2F_-}{d\eta_-^2}\right)^{\frac{1}{2}}\left(2F_- - \frac{3}{2}\eta_-\frac{dF_-}{d\eta_-}\right)^{\frac{1}{4}} e^{-T^2F_-(\eta_-)} \quad \text{as} \quad T \to -\infty \tag{A3.19}$$

completing the specification of the canonical 'diffraction' problem.

Since

$$\frac{d}{dT}\int_0^\infty X v_0(X,T)dX = v_0(0,T),$$

it follows from (A3.16) and (A3.19) that

$$\int_0^\infty X v_0(X,T)dX \to \left(\frac{\pi}{2p^{*3}}\right)^{\frac{1}{2}} \quad \text{as} \quad T \to +\infty$$

and hence that

$$v_0 \sim \frac{X}{(2p^*T)^{3/2}} e^{-X^2/4T} \quad \text{as} \quad T \to +\infty \quad \text{with} \quad X = O(T^{\frac{1}{2}}), \tag{A3.20}$$

wherein the exponential dependence is consistent with the second of (A3.9). In terms of the far-field behaviour, (A3.18) implies that

$$v_0 \sim \frac{1}{p^{*3/2}}\left(3\eta_+\frac{d^2F_+}{d\eta_+^2} - \frac{dF_+}{d\eta_+}\right)^{\frac{1}{2}}\left(\frac{3}{2}\eta_+\frac{dF_+}{d\eta_+} - 2F_+\right)^{\frac{1}{4}} e^{-T^2F_+(\eta_+)} \tag{A3.21}$$

for $X = O(T^{3/2})$ and the transition between (A3.20) and (A3.21) occurs over the scale $X = O(T)$: (A3.9) implies that (A3.21) has the asymptotic behaviour

$$v_0 \sim \frac{X}{2^{1/2}(p^*T)^{3/2}} e^{-X^2/4T} \tag{A3.22}$$

for $\eta_+ \ll 1$, so this transition is surprisingly subtle (it should be emphasised that it is clear *a priori* that (A3.22) need not be equivalent to (A3.20), since the ray solution is not of course an exact solution to the canonical inner problem – indeed (A3.21) would imply $v_0 = 0$ on $X = 0$, whereas (A3.19) satisfies the boundary condition (A3.16)). Thus in describing this transition we have

$$v_0 \sim \frac{1}{T^{1/2}} b\left(\frac{X}{T}\right) e^{X^2/4T} \quad \text{as} \quad T \to +\infty \quad \text{with} \quad X = O(T)$$

for some $b(\zeta)$ with

$$b(\zeta) \sim \frac{3}{(2p^*)^{3/2}} \quad \text{as} \quad \zeta \to 0, \; b(\zeta) \sim \frac{3}{2^{1/2} p^{*3/2}} \quad \text{as} \quad \zeta \to +\infty,$$

and construction of $b(\zeta)$ for $\zeta = O(1)$ would require the solution to (A3.12) subject to (A3.16) and (A3.19).

Finally, we note that the next term in the expansion

$$v \sim \; v_0(\hat{X}, T) + \varepsilon^{\frac{1}{4}} v_1(\hat{X}, T)$$

in $X < 0$ takes the form

$$v_1 = \frac{\varepsilon^{\frac{1}{4}}}{p^*} e^{p^* \hat{X}} \frac{\partial v_0}{\partial X}(0, T) \tag{A3.23}$$

where $v_0(X, T)$ is the solution to (A3.12), (A3.16), (A3.19): this induces an $O(\varepsilon^{\frac{1}{4}})$ correction term in v in $X > 0$ but, more importantly, confirms the applicability of the matching condition (A3.15). Given the exponential decay in T of (A3.14) and the algebraic decay of (A3.20), it is clear that (A3.23) becomes the dominant contribution to the reflected field for the large T.

REFERENCES

[1] J. K. Cohen and R. M. Lewis, *A ray method for the asymptotic solution of the diffusion equation*, IMA J. Appl. Math., **3** (1967), 266–290.

[2] C. M. Cuesta and J. R. King, *Front propagation a heterogeneous Fisher equation: The homogeneous case is non-generic*, Q. J. Mech. Appl. Math., **63** (2010), 521–571.

[3] U. Ebert and W. van Saarloos, *Front propagation into unstable states: Universal algebraic convergence towards uniformly translating pulled fronts*, Physica D, **146** (2000), 1–99.

[4] L. C. Evans and P. E. Souganidis, *A PDE approach to geometric optics for certain semilinear parabolic equations*, Indiana Uni. Math. J., **38** (1989), 141–172.

[5] J. Smoller, "Linear Elastic Waves," Cambridge University Press, 2001.

[6] M. Freidlin, *Limit theorems for large deviations and reaction-diffusion equations*, Ann. Prob., **13** (1985), 639–675.

[7] John King, "Mathematical Aspects of Semiconductor Process Modelling," DPhil Thesis, University of Oxford. 1986.

[8] J. R. King, *High concentration arsenic diffusion in crystalline silicon: An asymptotic analysis*, IMA J. Appl. Math., **38** (1987), 87–95.

[9] V. Méndez, J. Fort, H. G. Rotstein and S. Fedotov, *Speed of reaction-diffusion fronts in spatially heterogeneous media*, Phys. Rev. E, **68** (2003), 041105.

[10] A. I. Volpert, V. A. Volpert and V. A. Volpert, "Traveling Wave Solutions of Parabolic Systems," American Mathematical Society, 1994.

[11] J. Xin, *Front propagation in heterogeneous media*, SIAM Rev., **42** (2000), 161–230.

Received March 2012; revised February 2013.

E-mail address: john.king@nottingham.ac.uk